The EMBO Journal Vol.17 No.24 pp.7320–7336, 1998

A cdc15-like adaptor protein (CD2BP1) interacts with the CD2 cytoplasmic domain and regulates CD2-triggered adhesion

Jing Li[1,2], Kazuhisa Nishizawa[1,2], Wenqian An[1,2,3], Rebecca E.Hussey[1,4], Faye E.Lialios[1], Ravi Salgia[2,5], Raute Sunder-Plassmann[1,2,6] and Ellis L.Reinherz[1,2,7]

[1]Laboratory of Immunobiology and [5]Department of Adult Oncology, Dana-Farber Cancer Institute, and Departments of [2]Medicine and [4]Pathology, Harvard Medical School, 44 Binney Street J318, Boston, MA 02115, USA

[3]Present address: Millenium Pharmaceuticals, 640 Memorial Drive, Cambridge, MA 02139, USA
[6]Present address: Department of Internal Medicine III, University of Vienna, Vienna, Austria

[7]Corresponding author

A human CD2 cytoplasmic tail-binding protein, termed CD2BP1, was identified by an interaction trap cloning method. Expression of CD2BP1 is restricted to hematopoietic tissue, being prominent in T and natural killer (NK) cells, with long (CD2BP1L) and short (CD2BP1S) variants arising by alternative RNA splicing. Both CD2BP1 molecules are homologous to *Schizosaccharomyces pombe* cdc15, and include a helical domain, variable length intervening PEST sequence and C-terminal SH3 domain. Although the CD2BP1 SH3 domain binds directly to the CD2 sequence, KGPPLPRPRV (amino acids 300–309), its association is augmented markedly by the CD2BP1 N-terminal segment. Upon ligand-induced clustering of surface CD2 molecules, CD2BP1 redistributes from a cytosolic to a surface membrane compartment, co-localizing with CD2. In turn, CD2-stimulated adhesion is down-regulated by CD2BP1, apparently through coupling of the protein tyrosine phosphatase (PTP)-PEST to CD2. These findings offer the first molecular view into the control processes for T cell adhesion.

Keywords: adhesion/CD2/protein tyrosine phosphatase/SH3 domains/signal transduction

Introduction

The human CD2 molecule is found on virtually all T cells and thymocytes as well as on natural killer (NK) cells, and binds to the surface glycoprotein CD58 which is present on many cell types including antigen-presenting cells (APCs) (Sanchez-Madrid *et al*., 1982; Krensky *et al*., 1983; Selvaraj *et al*., 1987; Bierer *et al*., 1989; Moingeon *et al*., 1989a; Springer, 1990). CD2 promotes the initial stages of T cell contact with a cognate partner such as an APC even prior to T cell receptor (TCR) recognition of a peptide antigen bound to a major histocompatibility complex (MHC) molecule (Moingeon *et al*., 1989a,b; Koyasu *et al*., 1990). This makes the antigen recognition process much more efficient, by increasing the dwell time when opposing cellular plasma membranes are in contact and, thus, offering a greater opportunity for an individual TCR to locate an MHC molecule complexed with a specific antigenic peptide. While it is known that the monomeric affinity of the CD2–CD58 interaction is low (K_d = μM), co-ligation of CD2 and CD58 molecules on opposing cells within a conjugate pair induces CD2 redistribution to the region of cell–cell contact, resulting in a substantial avidity boost (Sayre *et al*., 1989; Koyasu *et al*., 1990; Recny *et al*., 1990; Arulanandam *et al*., 1993a; Li *et al*., 1996).

Considerable structural detail exists regarding CD2 and its CD58-binding site. Nuclear magnetic resolution studies of the N-terminal domain of rat and human CD2 (Driscoll *et al*., 1991; Withka *et al*., 1993) and X-ray crystallographic studies of the entire extracellular segment of rat and human CD2 (Jones *et al*., 1992; Bodian *et al*., 1994) have revealed that the extracellular segments consist of two immunoglobulin superfamily (IgSF) domains: a nine-stranded N-terminal V set domain lacking the first half of strand A, and a seven-stranded membrane-proximal C2 set domain. Prior studies have shown that the N-terminal membrane-distal domain (D1) mediates the adhesion function of the molecule by binding to the relevant counter-receptor (Sayre *et al*., 1989; Recny *et al*., 1990). Mutational analysis of human CD2 has demonstrated that the CD58-binding surface is located on the highly charged GFCC′C″ face of the protein (Peterson and Seed, 1987; Arulanandam *et al*., 1993b; Somoza *et al*., 1993; Osborn *et al*., 1995). Notably, this same surface area forms a homodimeric contact in the crystal structures of rat and human CD2 (Jones *et al*., 1992; Bodian *et al*., 1994). Further mutational studies in rat and human systems have suggested that the receptor–ligand interaction involves the major β-sheet surfaces of both CD2 adhesion and co-receptor domains (Arulanandam *et al*., 1994; van der Merwe *et al*., 1994).

CD2 functions as a signaling molecule in a number of important settings. First, CD58 interaction with CD2 augments interleukin-12 (IL-12) responsiveness of activated T cells with regard to proliferation and interferon-γ (IFN-γ) production (Wingren *et al*., 1993; Gollob *et al*., 1995, 1996). Second, the CD2–CD58 interaction has been reported to reverse T cell anergy (Boussiotis *et al*., 1994). Third, the CD2 cytoplasmic tail is required for optimal CD2 augmentation of antigen-triggered T cell responses (Moingeon *et al*., 1989b; Hahn and Bierer, 1993). Hence, in addition to augmenting antigen recognition via its role in adhesion, CD2 facilitates antigen recognition via signal transduction. Consistent with this notion is the fact that T cell proliferation in response to suboptimal concentrations of anti-CD3 monoclonal antibody (mAb) is augmented by CD2 cross-linking through addition of

specific pairs of anti-CD2 mAbs (Yang *et al*., 1986; Bierer *et al*., 1988). Furthermore, certain pairs of anti-CD2 mAbs can stimulate calcium flux, IL-2 production and cytolytic activity in and of themselves (Meuer *et al*., 1984; Siliciano *et al*., 1985).

Although the functional consequences of CD2–CD58 interaction vis-a-vis signaling are compelling, the molecular basis of CD2-mediated signal transduction is essentially unknown. Truncation and mutation of the CD2 cytoplasmic tail indicate that it is involved in the T cell activation process (Bierer *et al*., 1988; Chang *et al*., 1989; Hahn and Bierer, 1993). However, the lack of protein kinase or phosphatase domains or defined signaling motifs within the cytoplasmic tail has complicated the effort to understand the basis for CD2 signaling. It is noteworthy, however, that the positively charged CD2 cytoplasmic tail segment (pI ~12) contains 116 amino acids, 20% of which are prolines (Clayton *et al*., 1987; Sayre *et al*., 1987; Tavernor *et al*., 1994). One or more of these proline-rich segments may serve as a docking site for SH3 domains. To date, two reports have suggested that $p59^{fyn}$ and $p56^{lck}$ may be associated directly with the CD2 tail (Gassmann *et al*., 1994; Bell *et al*., 1996).

To define CD2 tail interaction proteins without restricting the search to known kinases, we have utilized a yeast interaction trap system (Finley and Brent, 1995) to screen a cDNA library derived from activated human T cells. One clone, termed CD2BP1, was shown to define a novel protein containing an SH3 domain which specifically associates with the CD2 tail. Moreover, this interactor appears to function as an adaptor to recruit the cytosolic protein tyrosine phosphatase (PTP)-PEST (Garton and Tonks, 1994) to the CD2 tail. In so doing, CD2-triggered adhesion involving CD58 as well as integrin-mediated adhesion activated via CD2 are both downregulated.

Results

Yeast two-hybrid screening of CD2 cytoplasmic tail interaction proteins

To identify proteins interacting with the CD2 cytoplasmic tail, we employed a yeast two-hybrid system using the full-length CD2 cytoplasmic tail cDNA sequence in pEG202 as bait and a T cell-derived cDNA library ligated into the pJG4-5 yeast vector (Finley and Brent, 1995). In this yeast interaction trap system, the CD2 tail cDNA (nucleotides 756–1076, amino acids 221–327) (Clayton *et al*., 1987; Sayre *et al*., 1987) is fused downstream of the DNA encoding the LexA promoter-binding domain in pEG202 such that the hybrid protein is constitutively expressed from an ADH1 promoter. Moreover, this protein can bind specifically to a promoter sequence containing a LexA-binding site. However, in the absence of an activation domain, transcription is not initiated. In parallel, individual inserts from the activated T cell-derived cDNA library were ligated into pJG4-5 downstream of the B42 transcription activation domain. Expression of this latter fusion protein is regulated by a GAL1 promoter such that its transcription is repressed in the presence of glucose but induced by galactose. In yeast, the interaction of the chimeric CD2 tail protein produced by pEG202 with a B42-cDNA fusion protein brings the B42 transcriptional activation domain close to the LexA-binding site on the colE1 LexA operator, resulting in activation of the downstream reporter gene [leucine (leu) synthetase or *lacZ*]. An interaction between the CD2 tail and any given cDNA product, therefore, can be detected as either yeast growth in leu^- medium or colonies showing blue color in the presence of X-gal under inductive conditions. As an additional control for the specificity of the binding of the cDNA-encoded protein to the CD2 cytoplasmic tail, a CD2 tail deletion construct was also engineered in pEG202 consisting of bp 756–854 (amino acids 221–253) and termed ΔCD2.

Of $\sim 7 \times 10^6$ yeast transformants screened in the CD2 tail interaction trap system, nine independent colonies containing distinct insert sizes were identified as positive. Among them, clone #48 (CD2BP1S) showed a strong and specific interaction. Thus, under galactose induction conditions, transformation of the CD2 tail/pEG202 and CD2BP1S/pJG4-5 plasmids (CD2/BP1) in yeast yielded double transformants positive for growth in leu^- medium and *lacZ* expression in leu^+ medium. In contrast, in the absence of induction (i.e. the presence of glucose), doubly transformed colonies showed neither growth in leu^- medium nor *lacZ* induction. These results indicate that the interaction between the hybrid CD2 tail protein and the CD2BP1 fusion protein is specific rather than a secondary effect of the CD2 tail fusion on yeast growth or *lacZ* expression. Furthermore, when the ΔCD2 construct was analyzed under the same conditions in either induced or uninduced states, the doubly transformed yeast (ΔCD2/BP1) gave negative results for both leu^- growth and *lacZ* expression. These findings demonstrate that CD2BP1 specifically interacts with the CD2 tail rather than another component of the fusion protein. Given that ΔCD2 encodes only the membrane-proximal 43 amino acids of the 116 amino acid CD2 cytoplasmic tail, which is itself incapable of mediating CD2-based signal transduction (Chang *et al*., 1989), this result suggests that CD2BP1 may be responsible for a critical component of the CD2 tail function.

Sequence analysis of CD2BP1 clones

DNA sequencing of the CD2BP1S cDNA fragment showed a 1578 bp insert containing several potential translation start codons close to the 5′ end of the sequence and a 3′ polyadenylation track (data not shown). None of the potential start codons showed a canonical Kozak sequence. In addition, because Northern analysis indicated that the size of the intact CD2BP1 mRNA was ~1.9 kb (see below) and there was an open reading frame (ORF) extending 5′ of the ATG in the cDNA insert, it was unclear whether the entire coding region of CD2BP1S had been cloned. Therefore, we performed 5′-RACE to define the entire coding region of *CD2BP1*. A 528 bp fragment RACE product (#17) including ~200 bp 5′ of the CD2BP1S cDNA clone was then sequenced. This analysis revealed that there was no putative start codon in this upstream 5′ sequence, but rather, two in-frame stop codons. From this analysis, we conclude that the ATG at bp 1–3 in the CD2BP1S clone represents the translation initiation site (amino acid 1). The amino acid sequence deduced from that cDNA is shown in Figure 1.

To verify the sequence of CD2BP1S, we synthesized an independent cDNA library derived from activated

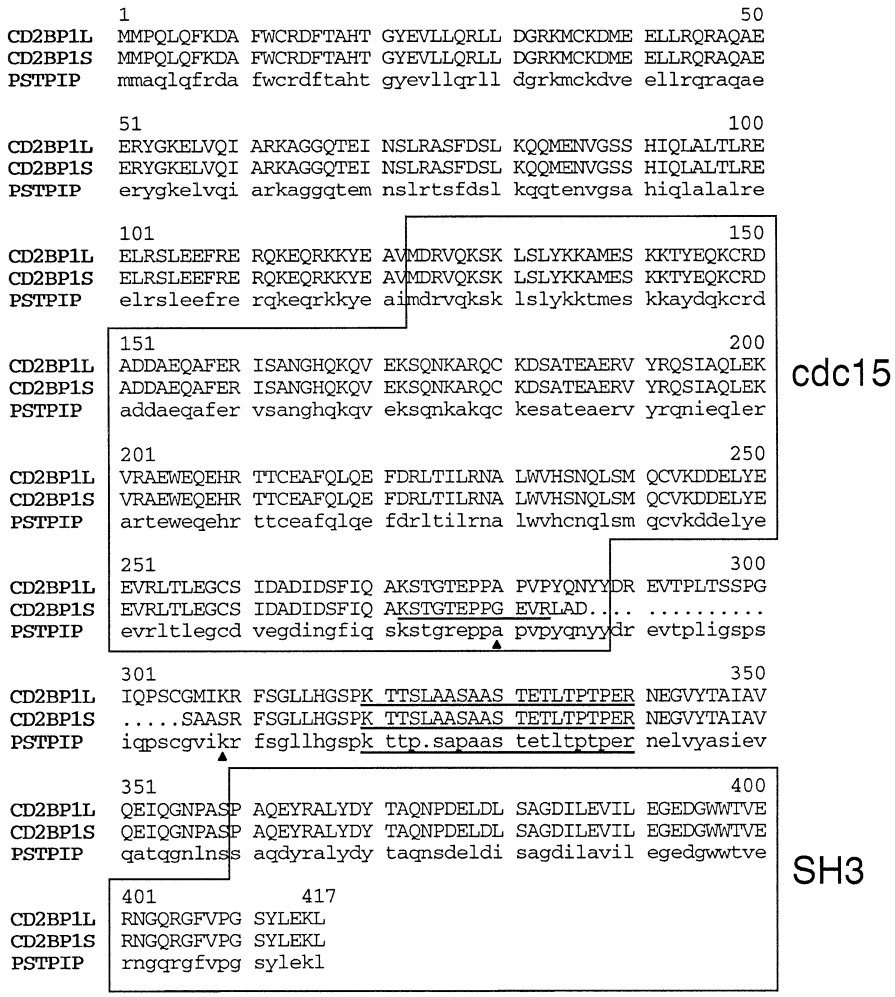

Fig. 1. Deduced amino acid sequences of CD2BP1L and CD2BP1S cDNAs. The sequences exhibiting high homology to yeast cdc15 and to a typical SH3 domain are boxed. Potential PEST (Pro, Glu, Ser and Thr)-rich regions are underlined. Alignment was prepared using the GCG program (Group, 1991). Solid triangles denote the beginning and end of the segments with differing amino acid sequences in CD2BP1S and CD2BP1L. The murine homolog (PSTPIP) (Spencer *et al*., 1997) is shown in lower case letters.

T cells and screened it using a 1 kb CD2BP1S cDNA *Xho*I fragment. One clone among several, termed CD2BP1L, was isolated with an almost identical sequence to that of CD2BP1S. However, nucleotides 838–870 of CD2BP1S cDNA were replaced by a distinct 89 nucleotide segment (bp 838–927) in the CD2BP1L cDNA (Figure 1). Analysis of the nucleotides flanking this 89 bp sequence of CD2BP1L and the 32 bp sequence of CD2BP1S identified splice junction donor and acceptor sites, strongly implying that CD2BP1L and CD2BP1S are RNA splice variants derived from a single *CD2BP1* gene. The deduced amino acid sequence of CD2BP1L (Figure 1) shows 30 amino acids (residues 280–309) which are replaced by 11 amino acids (residues 280–290) in CD2BP1S.

Amino acid sequence analysis of CD2BP1L and CD2BP1S by BLAST homology search (Altschul *et al*., 1990) and visual inspection identified three striking features in these gene products. First, amino acids 123–288 of CD2BP1L show significant (30%) sequence identity with *Schizosaccharomyces pombe* cdc15 (Fankhauser *et al*., 1995). PAIRCOIL program analysis of the CD2BP1L and CD2BP1S sequences reveals a potential coiled-coil structure located within this region of the protein (amino acids 162–204 with score = 1.7–4.3) (Berger *et al*., 1995). Second, the search also identified the presence of an SH3 domain at the C-terminus of CD2BP1 (amino acids 360–416). This segment contains canonical features of all SH3 domains (A366, L367, Y368, D369, E377, G383, W396, W397, G406, P409 and Y412) (Musacchio *et al*., 1994; Guruprasad *et al*., 1995). Homology was also observed with SH3 domains of α-spectrin, α-fodrin, myosin heavy chain, abl interactor protein, human neutrophil cytosol factor 2, grb2 and phosphatidylinositol-3 kinase. It is noteworthy that a related C-terminal SH3 domain is found in *S.pombe* cdc15 and all cdc15 family members (Fankhauser *et al*., 1995). Third, a PEST-rich region (proline, glutamic acid, serine and threonine) is found between the more N-terminal cdc15-like domain and the SH3 domain (Rechsteiner and Rogers, 1996) in Figure 1. In CD2BP1L, this extends from residues 320 to 340. In CD2BP1S, as a consequence of RNA splicing variation, there are two PEST sequences, amino acids 272–283 and 301–321. More recent BLAST search analysis identified a murine CD2BP1L homolog (88% identity) (gi/1857712) of functional relevance in

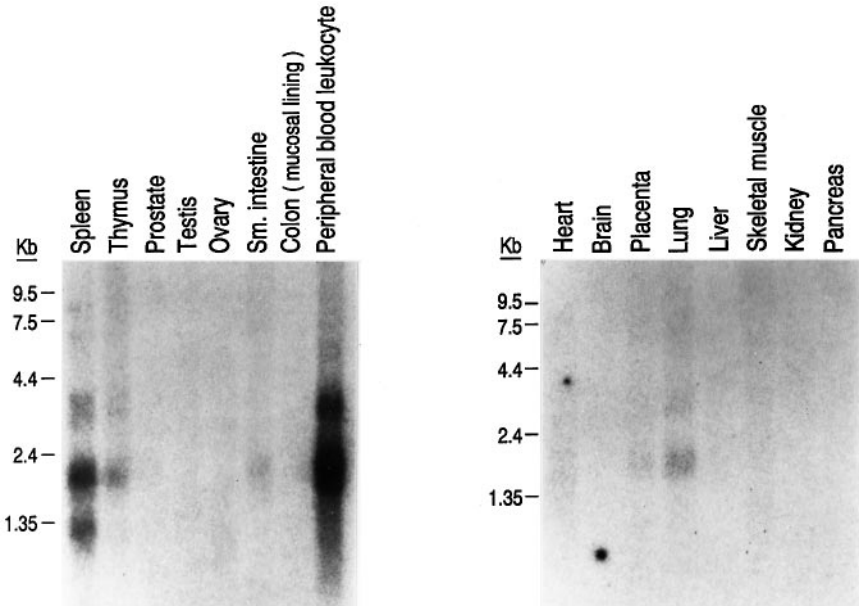

Fig. 2. *CD2BP1* gene expression in hematopoietic tissues. Northern hybridization of CD2BP1 cDNA to poly(A)$^+$ RNA from different human tissues shows preferential gene expression in hematopoietic-related tissues. The relative migration distances of RNA molecular weight markers are shown on the left side of each panel.

hematopoietic cells as reported by Lasky and colleagues (Spencer *et al*., 1997; Dowbenko *et al*., 1998; Wu *et al*., 1998).

CD2BP1 is expressed in hematopoietic tissues and prominently represented in mature T cells and NK cells

To next determine the expression pattern of the *CD2BP1* gene, Northern blot analysis was performed on poly(A)$^+$ RNA derived from a variety of different human organs using the 1 kb *Xho*I fragment of *CD2BP1* as a probe. As shown in Figure 2, the expression of CD2BP1 is largely restricted to the hematopoietic tissues, being prominent in spleen and peripheral blood leukocytes, with an estimated molecular RNA size of ~1.9 kb. Thymus, small intestine, lung and placenta show very low levels of expression, while no message is detected in prostate, testes, ovary, colon, heart, brain, liver, skeletal muscle, kidney or pancreas. Although not shown, analysis of human resting and activated T cells as well as the NKL IL-2-dependent human NK cell line showed a prominent 1.9 kb band. Detectable but low levels of CD2BP1 message are present in thymocytes and in the Epstein–Barr virus (EBV)-transformed B lymphoblastoid cell line, Laz509. In contrast, the non-hematopoietic HeLa human tumor line lacks CD2BP1 message. Collectively, the restricted expression pattern of CD2BP1 supports the notion that this gene product may be important in hematopoietic cell function and, more specifically, in development and/or activation of mature T and NK cells. It is noteworthy that the reported mRNA distribution of the murine homolog is broader (Spencer *et al*., 1997).

Comparison of steady-state CD2BP1 expression in resting versus activated human T cell populations demonstrates an increase in CD2BP1 message level following 3 days of activation by anti-CD3 mAb plus phorbol 12-myristate 13-acetate (PMA). Using reverse PCR and specific primers covering the junctional differences between CD2BP1L and CD2BP1S, we observed no detectable alterations in relative expression of the RNA splice variants in resting versus activated T cells. However, CD2BP1L was clearly the predominant isoform in both cases (data not shown). A less intense ~3.6 kb band is observed in activated T cells and is also observed in Northern blots using poly(A)$^+$ RNA (Figure 2). Presumably this band represents an alternative polyadenylated message, either a pre-mRNA or a mature splicing variant.

The CD2BP1 SH3 domain interacts directly with the CD2 cytoplasmic tail

Given that the predicted CD2BP1 protein sequence contains a C-terminal SH3 domain and that the CD2 cytoplasmic tail includes several proline-rich segments to which an SH3 domain might bind, we next examined the possibility that the CD2BP1 SH3 domain is necessary and sufficient for binding to the CD2 tail. To this end, a cDNA encoding the SH3 region (bp 1024–1382 of CD2BP1S) was obtained by PCR and inserted into the *Eco*RI and *Xho*I sites of the pGEX4T-1 GST expression vector. Purified GST or GST–CD2BP1SH3 fusion protein were incubated with lysates of activated human T lymphocytes as described in Materials and methods. The precipitates were subjected to SDS–PAGE, and the CD2 association with the CD2BP1SH3 domain revealed by Western blotting with polyclonal anti-CD2 heteroantisera (M32B) raised against the recombinant hCD2 ectodomain. As a positive control, lysates were immunoprecipitated with the anti-CD2 mAb 3T48B5 (Meuer *et al*., 1984) and then subjected to the same Western blot analysis. Figure 3A shows the results of one of three representative binding studies. The broad band in the 50–60 kDa range observed in the anti-CD2 immunoprecipitate is consistent with the known size of the glycosylated CD2 monomer (Sayre *et al*., 1987; Seed and Aruffo, 1987). Note that the 100–120 and 200 kDa bands probably represent CD2 oligomers. More importantly, in the presence of divalent cations, Zn^{2+},

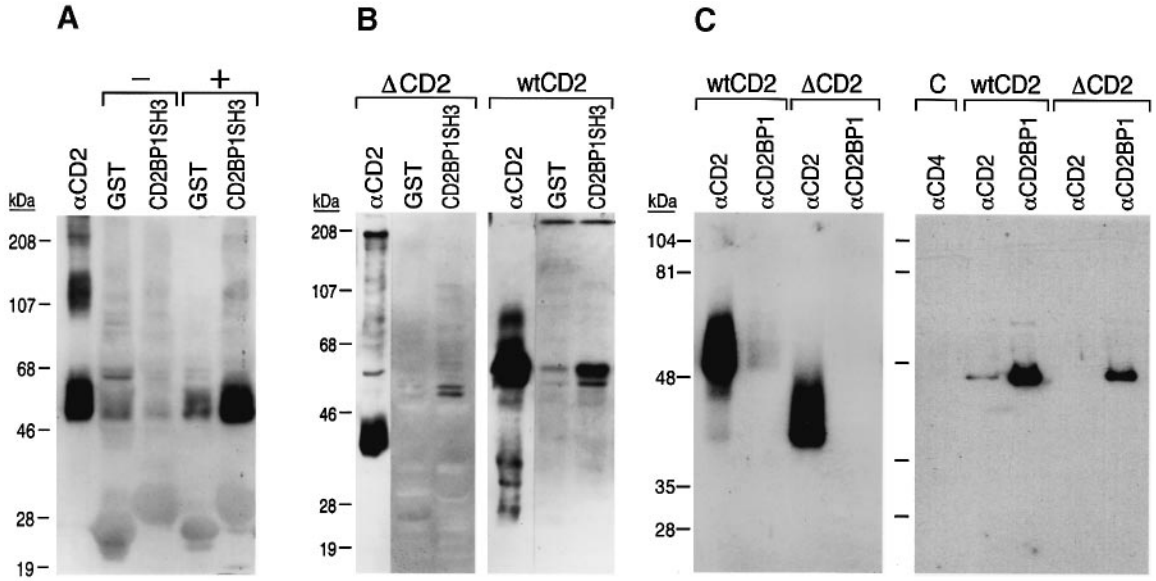

Fig. 3. Interaction of CD2BP1 with the CD2 cytoplasmic tail. (**A**) Western blot hybridization detects a specific interaction between CD2 in T cell lysates and the GST–CD2BP1SH3 fusion protein using M32B heteroantisera. αCD2, complexes precipitated by CNBr–Sepharose 4B beads coupled with anti-human CD2 mAb $T11_1$ (positive control); GST, complexes precipitated by glutathione–Sepharose 4B beads coupled with GST-binding protein (negative control); CD2BP1SH3, complexes precipitated by glutathione–Sepharose 4B beads coupled with GST–CD2BP1SH3 fusion protein. Precipitations were performed in the absence (–) of any extra bivalent ion or in the presence (+) of 200 μM Zn^{2+}. The relative migration distances of standard protein molecular weight markers (Bio-Rad) are shown on the left. (**B**) Western hybridization detects a specific interaction between GST–CD2BP1SH3 proteins and CD2 in the mouse T cell hybridoma 155.16 transfected with full-length human CD2 (W33) but not with a truncated human variant form (Δ25-2) (Li *et al*., 1996). αCD2, GST and CD2BP1SH3 lane are labeled as in (A). (**C**) Western blot analysis of immunoprecipitates from COS7 cells co-transfected with FLAG-tagged CD2BP1 and either wtCD2 or ΔCD2 (tailless variant) using anti-CD2 or anti-CD2BP1 mAbs. For blotting reagents, either anti-CD2 heteroantisera (left) or anti-FLAG mAb (right) were employed.

Mg^{2+} or Ca^{2+} at 2 μM to 2 mM concentrations (Figure 3A and data not shown), CD2 is immunoprecipitated with the CD2BP1SH3 fusion protein, but not by GST alone. Moreover, in the absence of divalent cations, no GST–CD2BP1SH3 interaction with CD2 is observed. This result is of note since earlier sequence analysis of the CD2 tail raised the possibility that it might contain a cation-binding site (Chang *et al*., 1989, 1990).

To verify further the specificity of the CD2 tail interaction with the CD2BP1SH3 domain, cell lysates were prepared from the mouse T cell hybridoma cells W33 (wtCD2) and Δ25-2 (ΔCD2), representing variants of the 155.16 cell line which were retrovirally transduced with wild-type human CD2 or a CD2 cytoplasmic tail-minus variant, respectively (Li *et al*., 1996). As expected, the GST–CD2BP1SH3 protein specifically interacts with the intact CD2 molecule in wtCD2 but not the tail-truncated CD2 molecule ΔCD2 (Figure 3B).

In parallel transient transfection experiments, the interaction between CD2BP1 and the CD2 tail was confirmed in COS7 cells using wtCD2 or ΔCD2 cDNA constructs co-transfected with FLAG-tagged CD2BP1L. As shown in Figure 3C (left panel) the anti-CD2BP1 mAb 8C93D8 (described in detail below) co-precipitated wtCD2 but not ΔCD2 protein. While the amount of CD2 is low compared with that detected in the 3T48B5 anti-CD2 mAb immunoprecipitation, the difference probably reflects the weak association between CD2 and CD2BP1 molecules. This result is corroborated in reciprocal co-precipitation analysis of CD2BP1 by anti-CD2 in wtCD2/CD2BP1 co-transfected COS7 cells but not in ΔCD2/CD2BP1 co-transfected COS7 cells (Figure 3C, right panel).

Localization of the CD2BP1-binding site on the CD2 cytoplasmic tail

There are five proline-rich (PXXP) segments within the CD2 tail (Figure 4A). Previous studies have indicated that in human CD2, the two most N-terminal sequences (PPPGHR) are necessary for signal transduction resulting in CD2-triggered IL-2 production (Chang *et al*., 1989; Hahn and Bierer, 1993). While the function of the others is yet to be defined, it is noteworthy that the C-terminal two proline-rich segments fall within a sequence of 18 amino acids, which is the most highly conserved CD2 cytoplasmic tail region across all species studied to date (Clayton *et al*., 1987; Tavernor *et al*., 1994). Given the likelihood that the CD2BP1 protein would interact with one of the proline-rich segments via its SH3 domain, we constructed by PCR different truncation variants of the CD2 tail in the yeast vector described above to pinpoint the site of the CD2BP1 SH3 interaction. Hence, construct N contains only the most N-terminal PPPGHR motif, construct M contains both PPPGHR sequences, construct L contains a proline-rich sequence (PPAP) in addition to the PPPGHR motifs but lacks the C-terminal conserved region, and construct K contains all but the C-terminal half of the most conserved sequence. These tail variants were tested in the yeast two-hybrid system for their interaction with CD2BP1L or CD2BP1S as well as truncations of the latter lacking the SH3 domain (CD2BP1S/ΔSH3) or consisting of the SH3 domain plus 34, 66 or 83 N-terminal residues ($SH3_{34}$, $SH3_{66}$ or $SH3_{83}$, respectively) or the SH3 domain alone with an artificial N-terminal linker ($SH3_{GGGGS}$) (Figure 4B). The strength of the interaction was determined by *lacZ* induction.

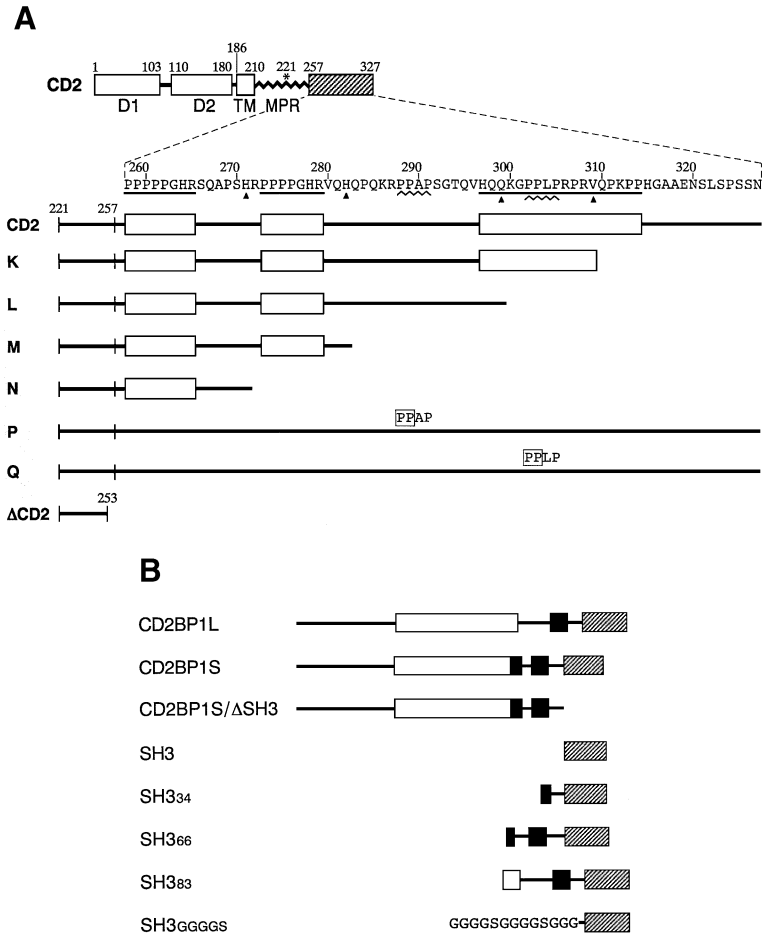

Fig. 4. Schematic representation of mutational variants of the CD2 cytoplasmic tail and the CD2BP1 protein characterized in yeast complementation assays. (**A**) Different CD2 tail truncation or mutation constructs (in pEG202) used in the yeast interaction system are shown. D1 and D2, domain 1 and domain 2 of the extracellular fragment of CD2, respectively; TM, the transmembrane segment of CD2; MPR, the membrane-proximal region of the CD2 tail. The amino acid numbers corresponding to each fragment are shown. All of the different CD2 tail variants in the pEG202 fusion include amino acids 221–257, except ΔCD2 as indicated. The three proline-rich regions conserved among species are underlined. Two of the proline-rich sequences are indicated by zig-zag lines. Different truncated fragments are shown with their truncation sites labeled as solid triangles under the sequence. The last amino acid of each variant includes the residue denoted by the solid triangle. Two prolines (boxed) were removed from the PPAP sequence in construct P and two prolines were removed from the PPLP sequence in construct Q. (**B**) CD2BP1 truncation constructs (in pJG4-5) used in the yeast interaction system. Open bars represent the region of CD2BP1 sequence with homology to yeast cdc15 protein amino acids 116–277. Solid bars represent PEST-rich regions in the CD2BP1 sequences. Hatched bars represent the SH3 domain in the CD2BP1 sequences. $SH3_{34}$ includes the entire SH3 domain of CD2BP1S and 34 N-terminal amino acids. $SH3_{66}$ includes the SH3 domain of CD2BP1S and 66 N-terminal amino acids. $SH3_{83}$ includes the SH3 domain of CD2BP1L and 83 N-terminal amino acids of CD2BP1L. $SH3_{GGGGS}$ includes the entire SH3 domain of CD2BP1 and an artificial linker consisting of the residues shown.

Table I. Mapping of the interaction between the CD2 cytoplasmic tail and CD2BP1 in a yeast two-hybrid system

	CD2[a]	K	L	M	N	P	Q	ΔCD2
CD2BP1S	++++[b]	++++	–	–	–	++++	++	–
CD2BP1L	++++	++++	–	–	–	++++	++	–
CD2BP1S/ΔSH3	–	–	–	–	–	–	–	–
$SH3_{34}$	+	+	–	–	–	+	–	–
$SH3_{GGGGS}$	+	+	–	–	–	+	–	–

[a]Different CD2 tail truncation constructs illustrated in Figure 4A and CD2BP1 constructs illustrated in Figure 4B are shown.
[b]Symbols indicate the strength of interaction between the corresponding regions of CD2 and CD2BP1 as detected by *lacZ* expression in the yeast system.

As summarized in Table I, the CD2BP1 protein interacts with the CD2 tail in the region between amino acids 300 and 309. Hence the K mutant is fully active while the L mutant has lost all activity. Consistent with this notion, deletion of proline residues 302 and 303 results in a marked attentuation of the intermolecular interaction (Figure 4A, construct Q). By contrast, comparable deletion of the proline residues 288 and 289 is without effect (Figure 4A, construct P). As expected, the more extensive CD2 truncations, M and N, are unable to interact with CD2BP1. Analysis of the CD2BP1S variants clearly shows that the CD2BP1 SH3 domain is essential for interaction with the

CD2 cytoplasmic tail; CD2BP1S/ΔSH3 cannot interact with CD2. Notwithstanding this, the CD2BP1 SH3 domain ($SH3_{34}$) alone interacts only weakly with the CD2 tail. This weak interaction is not secondary to an inhibitory effect of the CD2BP1 sequences immediately N-terminal to its SH3 domain, since removal of these residues and replacement with a synthetic linker, $SH3_{GGGGS}$, fails to augment the response.

Production of mAbs with specificity for CD2BP1 and identification of a 50 kDa protein in T lymphocytes

To characterize further the structure and function of CD2BP1, mAbs were generated against its SH3 domain. For this purpose, the GST–CD2BP1SH3 domain fusion protein was used to immunize Balb/C mice repeatedly. Subsequently, the immunized splenocytes were fused with NS1 myeloma cells, and hybridoma clones screened by enzyme-linked immunosorbent assay (ELISA) for production of mAbs reactive with plate-bound GST–CD2BP1SH3 protein but not plate-bound GST alone. Of the ~1600 primary clones screened, four (1E65B4, 8C93D8, 9B411F9 and 10C24B7) showed selective specificity for the GST–CD2BP1SH3 fusion protein. Antibody isotypes were determined by the Ouchterlony method: 1E65B4 and 10C24B7 belong to the IgM subclass, 9B411F9 belongs to the IgG1 subclass, and 8C93D8 belongs to the IgG2a subclass. Binding studies show that the relative affinity of the 8C93D8 is 150- to 200-fold better than that of the other mAbs (data not shown). Consistent with this observation, only 8C93D8 was able to immunoprecipitate the ~50 kDa CD2BP1 protein from T cell lysates (data not shown).

Clustering of CD2 by CD58 or anti-CD2 mAbs induces the association of CD2BP1 with CD2 in T lymphocytes

Both the above biochemical studies with the GST–CD2BP1SH3 fusion protein and the genetic complementation analysis indicate a direct association between the CD2 cytoplasmic tail and the CD2BP1 protein. To determine the nature of the intermolecular interaction which occurs during physiological situations *in vivo*, we performed a series of immunofluorescence co-localization studies. To this end, activated human T cells were analyzed for CD2 and CD2BP1 expression, and the distribution pattern of these molecules on the T cell surface and within the T cell was compared prior to and following CD2 ligation. Fluorochrome-labeled mAbs specific for the extracellular adhesion domain of CD2 (anti-$T11_1$ Texas red or anti-$T11_3$ Texas red) were used to detect CD2 on the cell surface, and the CD2BP1 SH3-specific mAb 8C93D8–fluorescein isothiocyanate (FITC) was used for intracellular localization of CD2BP1. As shown in Figure 5c, the staining of CD2 on activated T cells gives a characteristic rim-like pattern representing a broad surface membrane distribution. In contrast, staining of CD2BP1 with 8C93D8 exhibits a diffuse intracellular staining pattern, a lack of nuclear staining and a weak surface membrane reactivity (Figure 5b). This result indicates that the CD2BP1 protein localizes mainly to the cytosol of the T cell. On the other hand, when CD2 molecules are cross-linked by anti-CD2 mAbs (anti-$T11_2$ + anti-$T11_3$ Texas red), they redistribute in clusters on the T cell surface (Figure 5g). Moreover, the staining pattern of CD2BP1 changes substantially. The previously rather uniform CD2BP1 cytoplasmic distribution becomes clustered near the cell surface membrane as well, with the CD2BP1 staining now co-localizing with the surface CD2 staining (Figure 5). This overlap is visualized readily as yellow staining given that the combination of Texas red CD2 staining and green FITC–CD2BP1 staining overlap (compare Figure 5d and h). A comparable redistribution of CD2BP1 was not observed after CD28 or TCR cross-linking with 9.3 anti-CD28 and RW28C8 anti-CD3ε mAb, respectively (data not shown).

To determine next whether binding of CD58 to the CD2 ectodomain might induce the association of CD2BP1 with CD2, cell–cell conjugates were formed between CD2-expressing activated T cells and human CD58-transfected CHO cells and the distribution of the CD2 and CD2BP1 proteins examined. As shown in Figure 5, when human CD58-transfected CHO cells interact with T cells, the CD2 redistributes on the T cell surface to the region of the cell–cell interaction interface, consistent with our prior results (Figure 5k) (Li *et al*., 1996). More importantly, the CD2BP1 protein reorganizes into the area of cell–cell contact as well (Figure 5j and l). The co-localization of CD2 and CD2BP1 following CD2 cross-linking by specific anti-CD2 mAbs or the CD58 ligand itself supports the conclusion that CD2 and CD2BP1 associate with one another during specific *in vivo* conditions in T lymphocytes. Furthermore, it is clear that this association is predominantly not constitutive but rather induced by ligation of the CD2 ectodomain. To some extent, even T cell–T cell interaction induces co-localization (Figure 5d). Analysis of the murine CD2BP1 homolog in 3T3 cells previously showed co-localization with cortical actin cytoskeleton, lamellipodia and the actin-rich cytokinetic cleavage furrow (Spencer *et al*., 1997).

CD2BP1 associates with the protein tyrosine phosphatase (PTP)-PEST

The CD2 cytoplasmic tail is known to be critical for signal transduction following ligation of the CD2 ectodomain (Chang *et al*., 1989; Hahn and Bierer, 1993). Given that the CD2 tail lacks a kinase or phosphatase domain, the most plausible way through which it might exert its effect on cellular activation is via coupling to a second signaling molecule. In principle, this might either be through a direct coupling between the CD2 tail and an enzyme or, alternatively, by an intermediate adaptor protein which interacts with CD2 and in turn couples to a kinase or phosphatase. The specific association of CD2BP1 with CD2 both *in vitro* and *in vivo* suggests that it is a possible candidate for such a coupling component. Since the amino acid sequence of CD2BP1 shows it to have neither a kinase nor a phosphatase domain, CD2BP1 probably subserves an adaptor function.

To test this possibility, 8C93D8 was used to immunoprecipitate CD2BP1 from activated human T cell lysates, and any associated kinase or phosphatase activity was determined by *in vitro* analysis. In immunoprecipitates made with an irrelevant mouse IgG control versus the CD2BP1-specific mAb, no serine-threonine kinase or tyrosine kinase activities were found using histone H1

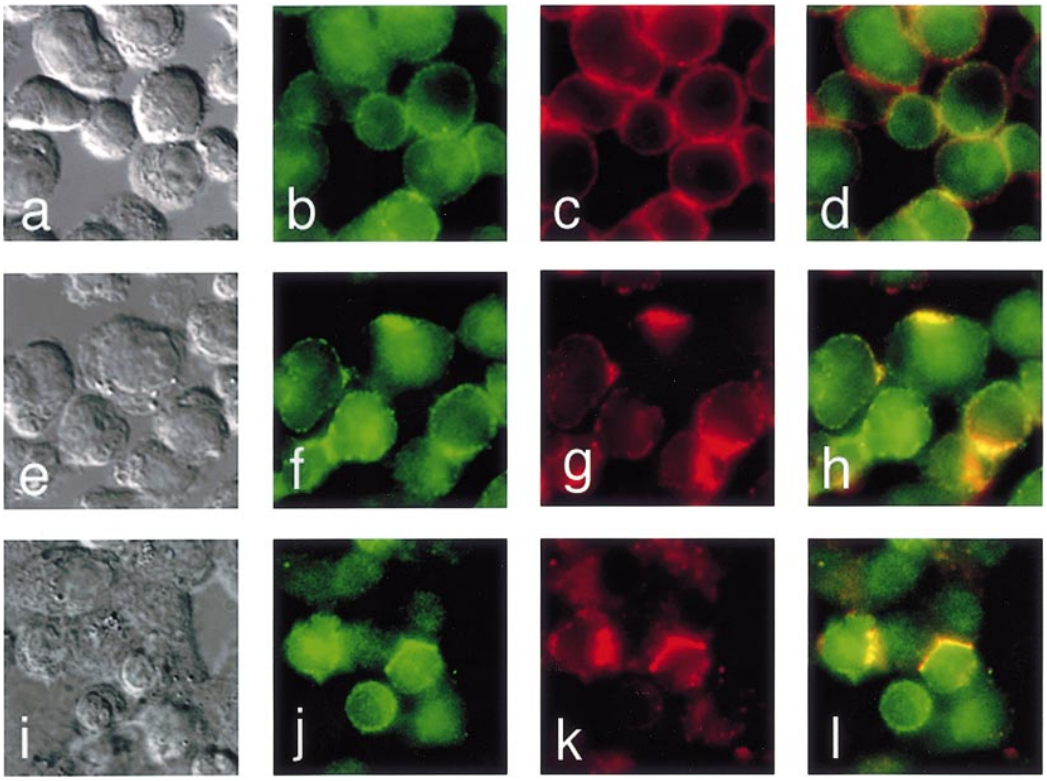

Fig. 5. Co-localization of CD2 and CD2BP1 following cross-linking of surface CD2 molecules. Fluorescence microscopic analysis of the distribution pattern of CD2BP1 and its co-localization with CD2 upon CD2 cross-linking. (**a**) Differential interference contrast (DIC) of activated human T cells. (**b**) FITC–anti-CD2BP1(8C93D8) staining, (**c**) Texas red–anti-CD2 ($T11_1$) staining and (**d**) FITC–anti-CD2BP1 and Texas red–anti-CD2 double staining of the same cells as in (a). (**e**) DIC of activated human T cells whose surface CD2 have been cross-linked by anti-CD2 antibodies anti-$T11_2$ and -$T11_3$. (**f**) FITC–anti-CD2-BP1 staining, (**g**) Texas red–anti-CD2 antibodies ($T11_3$) staining and (**h**) FITC–anti-CD2BP1 and Texas red-anti-CD2 double staining of the same cells as in (e). (**i**) DIC of activated human T cells forming conjugates with CHO/CD58 cells. (**j**) FITC–anti-CD2BP1 staining, (**k**) Texas red–anti-CD2 antibody ($T11_3$) staining and (**l**), FITC–anti-CD2BP1 and Texas red–anti-CD2 double staining of the same cells as in (i).

and Raytide or poly(Glu–Tyr), respectively, as substrates. However, in contrast to the lack of kinase activity, the CD2BP1 immunoprecipitates showed significant tyrosine phosphatase activity using phosphoRaytide as a substrate. This activity is illustrated as a linear time-dependent release of ^{32}P from tyrosine-phosphorylated Raytide. Moreover, sodium vanadate, the specific inhibitor of tyrosine phosphatases, blocks this reaction as expected (Figure 6).

Given the cytosolic distribution of CD2BP1, we investigated the possibility that a cytosolic PTP was the enzyme in question. To this end, we tested the association of CD2BP1 with the known cytoplasmic PTPs, PEST-PTP (Garton and Tonks, 1994), SHPTP1 (Matthews *et al*., 1992; Plutzky *et al*., 1992) and SHPTP2 (Freeman *et al*., 1992). We also tested FLP which, according to some studies, has a cytosolic distribution (Cheng *et al*., 1996; Dosil *et al*., 1996). For these experiments, activated T cell lysates were incubated with 8C93D8–Sepharose or control mouse IgG–Sepharose. Following immunoprecipitation and washing, the bead-bound material was subjected to SDS–PAGE, blotted to nitrocellulose membranes and incubated with polyclonal anti-PTP PEST (Garton and Tonks, 1994), anti-FLP (anti-EN12) (Dosil *et al*., 1996) or anti-SHPTP1 and anti-SHPTP2 antibodies (Freeman *et al*., 1992; Plutzky *et al*., 1992), and developed by ECL. Figure 6 (insert, lane 1) shows that in T cell lysates, the anti-PTP-PEST antisera detected a band at ~106 kDa which is the PTP-PEST protein (open arrowhead). The 8C93D8 anti-CD2BP1 mAb immunoprecipitates the same band, consistent with the notion that PTP-PEST and CD2BP1 co-associate (lane 6). The presence of PTP-PEST protein in the 8C93D8 immunoprecipitate is specific since no PTP-PEST protein band is observed in the mouse IgG–Sepharose immunoprecipitate (lane 7). To confirm further the specificity of the CD2BP1–PTP-PEST interaction, we examined whether excess soluble 8C93D8 or mouse IgG antibody pre-incubation with the T cell lysate could mediate specific inhibition of the immunoprecipitation by Sepharose-bound 8C93D8. As expected, pre-incubation with soluble mouse IgG had no effect on the PTP-PEST immunoprecipitation (lane 3). In contrast, pre-incubation of lysates with soluble 8C93D8 resulted in the inability of the 8C93D8–Sepharose to co-precipitate the PTP-PEST band (lane 2). Lanes 4 and 5 represent comparable controls for non-specific mouse IgG–Sepharose immunoprecipitation. Under either pre-incubation condition, no 106 kDa band is seen, as expected. The results of this soluble antibody competition assay further support the view that CD2BP1 associates specifically with PTP-PEST. Figure 6 also shows that in addition to the 110 kDa PTP-PEST band, the 8C93D8 also apparently immunoprecipitates a band at ~80 kDa from the T cell lysate which reacts with the anti-PTP-PEST antisera by Western blot (solid arrowhead). Whether this band represents a proteolytic product of PTP-PEST or a related

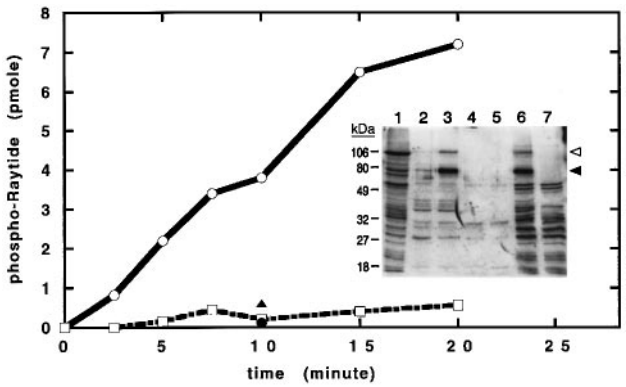

Fig. 6. Protein tyrosine phosphatase activity is associated with CD2BP1. Time course phosphatase assay reveals that the CD2BP1 immunocomplex is associated with protein tyrosine phosphatase activity. Solid line, assay on immunocomplexes immunoprecipitated by anti-CD2BP1; dotted line, assay on immunocomplexes precipitated by control mouse IgG. The solid triangle indicates 10 min assay reaction of anti-CD2BP1 immunocomplexes in the presence of the specific protein tyrosine phosphatase inhibitor sodium vanadate (1 mM). The solid circle indicates the value for the control mouse IgG immunocomplexes assayed under the same reaction conditions as for the solid triangle. The *y* axis represents pmol of ^{32}P released from phosphoRaytide and the *x* axis represents time. Results are representative of three independent experiments. Insert: CD2BP1 associates with PTP-PEST. Western hybridization using CSH8 anti-PTP-PEST rabbit heteroantisera detects PTP-PEST in immunocomplexes precipitated specifically by anti-CD2BP1 beads. Lane 1, total lysate from activated human T cells; lane 2, immunocomplexes precipitated by anti-CD2BP1 beads in the presence of a 10-fold molar excess of soluble anti-CD2BP1; lane 3, immunocomplexes precipitated by anti-CD2BP1 beads in the presence of a 10-fold molar excess of soluble mouse IgG; lane 4, immunocomplexes precipitated by mouse IgG beads in the presence of a 10-fold molar excess of soluble anti-CD2BP1; lane 5, immunocomplexes precipitated by mouse IgG beads in the presence of a 10-fold molar excess of soluble mouse IgG; lane 6, immunocomplexes precipitated by anti-CD2BP1 beads in the absence of soluble antibody; lane 7, immunocomplexes precipitated by mouse control IgG beads in the absence of soluble antibody.

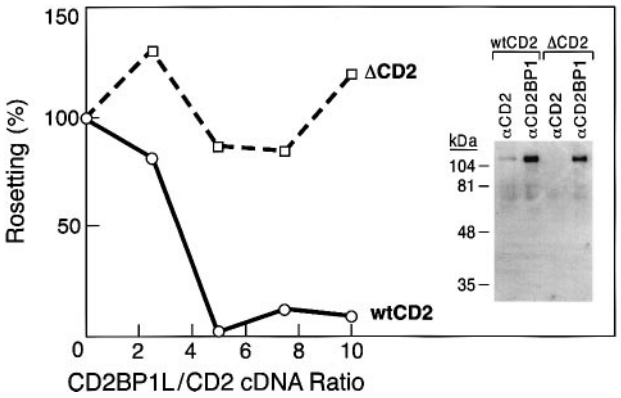

Fig. 7. CD2BP1 downregulates CD2-mediated cell–cell adhesion. A 0.5 μg aliquot of wtCD2 or ΔCD2 in the CDM8 expression vector was co-transfected with 1.25, 2.5, 3.75 and 5 μg of CD2BP1L into COS7 cells. Subsequently, each transfection was assayed for rosetting with SRBCs at room temperature as an indicator of CD2–CD58 interaction. wtCD2 (○) rosetting decreases with increased CD2BP1L cDNA co-transfection whereas tail-truncated ΔCD2 (□) rosetting does not change. Insert: anti-PTP-PEST Western blot of immunoprecipitates from wtCD2 + CD2BP1- or ΔCD2 + CD2BP1-transfected cells using the indicated mAbs.

but distinct PTP remains to be determined. Parallel analysis of these same lysates and immunoprecipitates with other PTP-specific reagents failed to show any specific association of SHPTP1, SHPTP2 or FLP with the CD2BP1 protein (data not shown).

The CD2BP1 adaptor functions as a negative regulator of CD2-stimulated adhesion

Given the homology of CD2BP1 to cdc15, a protein involved in regulating cytokinesis through cytoskeletal interaction, it was possible that CD2BP1 might regulate cellular motility/adhesion. Having established an association between CD2BP1 and CD2, and between PTP-PEST and CD2BP1, we speculated that CD2BP1 might function as an adaptor to couple PTP-PEST to CD2. As such, this coupling may regulate CD2 function. For example, by binding to the most conserved CD2 tail segment, CD2BP1 would couple PTP-PEST to CD2. To examine this possibility, CD2 and CD2BP1 were introduced into COS7 cells and rosetting assays were performed between the CD2-expressed COS7 cells and sheep red blood cells (SRBCs) which express the CD2 ligand CD58. Because COS7 cells do not express endogenous CD2BP1 (our unpublished results), we used this system to study the effect of expression of CD2BP1 on CD2 rosette formation. Consequently, we transfected COS7 cells with a fixed amount of CD2 cDNA in conjunction with variable amounts of CD2BP1 cDNA under conditions where surface CD2 expression was essentially similar. As shown in Figure 7, with increasing expression of CD2BP1, the rosetting of wtCD2-expressing COS7 cells decreased by 90% despite a constant surface CD2 expression level as analyzed by anti-$T11_1$ mAb staining on FACS. This inhibitory effect of CD2BP1 almost certainly resulted from its association with the CD2 tail because when CD2BP1 was co-expressed with the ΔCD2 variant, there was no obvious reduction in rosetting. Figure 7 (insert) indicates that a fraction of PTP-PEST can be immunoprecipitated with anti-CD2 mAb from wtCD2 + CD2BP1 but not ΔCD2 + CD2BP1 co-transfectant COS7 cells. Nor could PTP-PEST be immunoprecipitated with anti-CD2 mAb from COS7 cells transfected with CD2 alone (data not shown). Together, these results indicate that one important role of the CD2BP1 association with the CD2 tail is to downregulate CD2-based cell adhesion. As discussed below in detail, dephosphorylation of cellular substrates probably modulates adhesion as known to be the case for focal adhesion processes.

It is known that CD2 signaling upregulates integrin-based cellular adhesion (Shimizu *et al.*, 1995). Hence, CD2BP1 may also function to regulate the CD2-triggered integrin pathway as well. To investigate this possibility, the Jurkat J77 human T cell line was employed as a recipient for transfection since it lacks CD2BP1 message (unpublished results). Specifically, CD2BP1 cDNA was transfected into J77 cells, and stable CD2BP1 expression transfectants were selected by FACS analysis and confirmed by Northern blot hybridization. Both negative control D5 (vector only) and CD2BP1 Jurkat transfectants were examined for their adhesion to fibronectin-coated surfaces before or after CD2 triggering through anti-$T11_2$ + anti-$T11_3$ mAb cross-linking. Representative results are illustrated for D5 and one of two representative CD2BP1 transfectants (Figure 8). As shown, prior to CD2 cross-linking, control (Figure 8a and b) and the CD2BP1

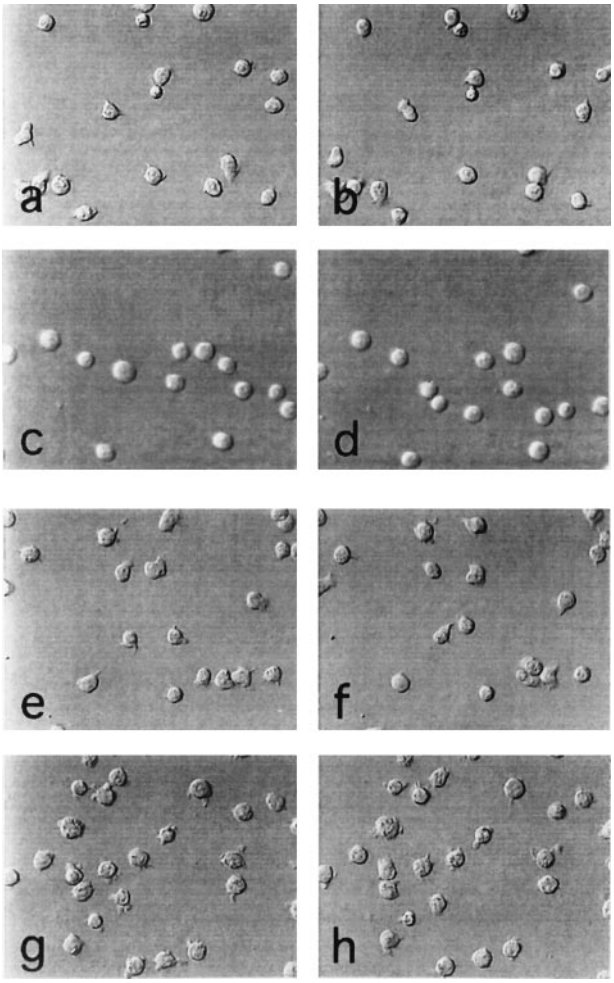

Fig. 8. Time-lapse video microscopy of CD2BP1 transfected Jurkat cells. As described in Materials and methods, mock-transfected (**a–d**) and CD2BP1-transfected Jurkat cells (**e–h**) were visualized by time-lapse video microscopy, without (a, b, e and f) and with CD2 cross-linking (c, d, g and h). Note how mock-transfected Jurkat cells had rounded morphology with less membrane ruffling and microspikes in response to CD2 cross-linking, whereas CD2BP1-transfected Jurkat cells did not change their cell morphology or motility in response to CD2 cross-linking.

transfectant (Figure 8e and f) exhibit comparable cellular motility on a fibronectin surface as evaluated by time-lapse photography. Representative membrane ruffling and protrusion/retractions, indicative of normal cytoskeletal function, was observed. However, within several minutes following CD2 cross-linking, the D5 and CD2BP1 transfectants exhibit significantly different cellular activities. As shown in Figure 8c and d, D5 cells lacking CD2BP1 became round and manifested no protrusion/retraction movements, thereby indicating the cessation of motility. In contrast, both CD2BP1 transfectants showed normal motility and filopodial formation (Figure 8g and h). These studies clearly indicate that CD2BP1 not only regulates CD2-based cellular adhesion events but also is involved in CD2 regulation of integrin-based movement. Hence, in the absence of CD2BP1, CD2-activated adhesion is dysregulated such that normal motility is interrupted.

Discussion

A yeast two-hybrid system was used to clone a novel molecule, CD2BP1, which specifically associates with the CD2 cytoplasmic tail in T lymphocytes. Biochemical studies map the interaction with CD2 to the SH3 domain in CD2BP1, a finding independently confirmed by genetic complementation analysis in yeast. Further mutational analyses localize the CD2BP1-binding site to the area centered about the PPLP sequence (amino acids 302–305) in the C-terminal region of the CD2 tail. This CD2 segment (amino acids 297–314) contains the sequence most highly conserved among CD2 homologs in all species (Clayton *et al*., 1987; Tavernor *et al*., 1994).

Experiments on rat CD2 have provided evidence that the region homologous to human CD2 amino acids 297–314 is capable of interacting with the SH3 domain of $p56^{lck}$ (Bell *et al*., 1996). Moreover, it is claimed that augmentation of human CD2–CD58 avidity by an inside-out signaling pathway functionally linked to the TCR involves a portion of this conserved region C-terminal to the PPLP site (Hahn and Bierer, 1993). The region important for CD2-based IL-2 production, however, lies outside the conserved C-terminal region. Previous human CD2 tail mutational studies defined the two PPPGHR sequences located within the N-terminal half of the CD2 tail (amino acids 260–265 and 274–279) as crucial for IL-2 production and calcium flux initiated through CD2 triggering. Thus, the CD2 cytoplasmic tail appears to contain several functional regions.

Paradoxically, there is no requirement for the CD2 cytoplasmic tail in CD2-mediated cell adhesion and ligand (CD58)-induced CD2 reorganization which occurs subsequent to T cell–APC conjugate formation (Koyasu *et al*., 1990; Li *et al*., 1996). A cytoplasmic tail deletion mutant of CD2 lacking the C-terminal 92 amino acids is still capable of relocalizing to the area of cell–cell interaction (Li *et al*., 1996). However, these studies do not rule out the possibility that the CD2 cytoplasmic tail is involved in the subsequent regulation of the adhesion complex. In this regard, the homology observed between the amino acid sequences of CD2BP1 and cdc15 (*S.pombe*) suggests that the function of these two molecules in the cell may be related. Cdc15 has been found to represent a critical component involved in cytoskeletal rearrangements related to actin ring formation during yeast cell division. Although the detailed mechanisms involving cdc15 function are yet to be determined, heavily phosphorylated cdc15 is detected during this process. The presence of multiple shared tyrosine residues in CD2BP1L and CD2BP1S suggests that by binding to the CD2 tail, CD2BP1 may regulate CD2-related cytoskeletal rearrangement events in a manner analogous to that of its cdc15 counterpart.

CD2–CD58-driven conjugate formation between T lymphocytes and APCs facilitates TCR-mediated antigen recognition of peptide/MHC ligands and, subsequently, the attendant downstream cellular activation events. For effective T lymphocyte function, the nature and duration of these cellular events require tight regulation. Hence, reversible adhesion must occur. Once activated CTLs detach from their cognate partners, they can recycle to address other target cells or undergo conversion to a quiescent state. The mechanisms regulating those

processes are yet to be elucidated. One important finding of our current research is that while CD2BP1 only transiently interacts with CD2, it nevertheless shows a stable association with PTP-PEST. The inducible binding of CD2BP1 to CD2 during CD2 cluster formation is probably essential for its normal adaptor function in recruiting PTP-PEST to the vicinity of the adhesion complex at the cell–cell junction, thereby downregulating adhesion following CD2–CD58 co-ligation. As shown by the motility and adhesion analysis of Jurkat T cell transfectants on fibronectin surfaces, CD2-activated integrin adhesion is also regulated by CD2BP1.

Tyrosine phosphorylation of macromolecules is important in many forms of signal transduction processes (Matsuzaki *et al*., 1993; Ihle *et al*., 1995; Swain and Cambier, 1996). The regulation of the phosphorylation status of the receptor as well as downstream molecules in the signaling pathway provide a common means for cascade signal amplification control. In the case of cell adhesion, accumulating data have uncovered the importance of tyrosine phosphorylation on components of adhesion complexes as a means of regulating complex formation and function (Kanner *et al*., 1991; Sakai *et al*., 1994; Vuori and Ruoslahti, 1995; Vuori *et al*., 1996; Nakamoto *et al*., 1997; Schlaepfer and Hunter, 1997). In this regard, the control of the level of tyrosine phosphorylation and dephosphorylation reactions by kinases and phosphatases, respectively, is central for signal transduction and cell adhesion events (Chow *et al*., 1993; Howell and Cooper, 1994; Liu *et al*., 1996; Tobe *et al*., 1996; Black and Bliska, 1997).

PTP-PEST is a widely expressed protein tyrosine phosphatase with a cytosolic distribution. It contributes >90% of the cytosolic tyrosine phosphatase activity in most cells and is maintained in a constantly active state (Garton *et al*., 1996). Recently, by using substrate-trapping techniques, it was reported that PTP-PEST manifests a very restricted substrate specificity towards the tyrosine-phosphorylated protein p130^{CAS} (Garton *et al*., 1996, 1997). The latter has been observed as a non-phosphorylated species in resting cells and participates in focal adhesion complex formation in a phosphorylated form upon activation either by integrin-mediated cell adhesion or oncogene-mediated cell transformation (Mayer and Hanafusa, 1990; Kanner *et al*., 1991; Nojima *et al*., 1995; Vuori and Ruoslahti, 1995; Petruzzelli *et al*., 1996; Salgia *et al*., 1996; Vuori *et al*., 1996; Astier *et al*., 1997). While the exact function of phosphorylated p130^{CAS} in the adhesion complex is unclear, it appears to play a role in the adhesion complex formation and stabilization by interaction with other constituents through its phosphotyrosine residues (Kanner *et al*., 1991; Sakai *et al*., 1994; Petruzzelli *et al*., 1996; Salgia *et al*., 1996; Vuori *et al*., 1996; Nakamoto *et al*., 1997). Since CD2BP1 interacts with both the transmembrane CD2 protein and the cytosolic PTP-PEST protein, it may be linked directly or indirectly to phosphorylated p130^{CAS} function. As shown here (Figure 6) and elsewhere (Koyasu *et al*., 1990; Li *et al*., 1996), as CD2 reorganizes into the cell–cell adhesion junction, it becomes highly concentrated. Through targeting to the CD2 tail, CD2BP1 appears to bring the associated PTP-PEST to the membrane in the region of cell–cell contact. This may facilitate the PTP-PEST's ability to dephosphorylate the phosphorylated p130^{CAS} in the focal adhesion complex, thereby downregulating the adhesion complex. Interestingly, a bacterial PTP (YopH) has been reported to dephosphorylate p130^{CAS} and cause destabilization of focal adhesions (Black and Bliska, 1997).

It is noteworthy that PTP-PEST recently has been found to associate with the inhibitory signaling molecule csk through the interaction of the proline-rich sequence of PTP-PEST with the csk SH3 domain (Davidson *et al*., 1997). Csk functions by phosphorylating the C-terminal regulatory tyrosine on src-kinase family members, thereby inactivating their enzymatic activity (Chow *et al*., 1993; Cloutier *et al*., 1995). csk has been reported to localize to focal adhesions via its SH2 and SH3 domain interaction with src (Howell and Cooper, 1994; Sabe *et al*., 1994). In turn, src is constitutively present in focal adhesions where it phosphorylates other components of the complex such as FAK and p130^{CAS} (Vuori and Ruoslahti, 1995; Vuori *et al*., 1996; Nakamoto *et al*., 1997). A direct interaction of csk with FAK and paxillin through the csk SH2 domain has also been reported (Bergman *et al*., 1995; Tobe *et al*., 1996). The concerted influences of csk and PTP-PEST may be critical for negatively regulating the formation and/or function of the adhesion complex.

PTP-PEST has also been reported to associate with shc and grb2, molecules important for T cell activation events (Habib *et al*., 1994; Charest *et al*., 1996, 1997). The biochemical significance of these associations currently is unclear. However, several reports indicate that shc and grb2 associate with FAK in focal adhesions to provide a link between the focal adhesion complex and downstream signaling (Schlaepfer *et al*., 1994; Vuori *et al*., 1996; Schlaepfer and Hunter, 1997). It seems likely that PTP-PEST might associate with membrane-localized shc or grb2 molecules and thereby modify them by a dephosphorylation reaction influencing the signal transduction pathways involving these molecules.

Consistent with the notion that an adaptor protein such as CD2BP1 might have an important function in regulating cellular activation/adhesion events, BLAST search subsequent to CD2BP1 cloning recently has identified a murine protein with 88% identity to human CD2BP1 (gi/1857712). This was cloned from mouse hematopoietic progenitor cells as a protein associated with the PTP-PEST-related enzyme PTP-HSCF (FLP) (Spencer *et al*., 1997). These studies and additional ones (Dowbenko *et al*., 1998) also showed that the murine adaptor homolog (PSTPTP) interacts through its N-terminal coiled-coil domain with the C-terminal 24 amino acids of the PTP. The latter segment is conserved in all three PEST-related phosphatases (PTP-PEST, PTP-PEP and PTP-HSCF), implying that, at least in the mouse, more than one member of the enzyme family may interact with the adaptor homolog (Spencer *et al*., 1997). Whether the N-terminal coiled-coil fragment of human CD2BP1 interacts with PTP-PEST to promote association remains to be determined, but is likely given conservation of the functionally important W232 residue in mouse and man (Dowbenko *et al*., 1998). The inability to detect an interaction between CD2BP1 and SHPTP1, SHPTP2 and FLP attests to the specificity of CD2BP1 interaction with PTP-PEST. As PTP-PEP is nuclear in localization, this phosphatase is unlikely to make a physiologically relevant link with

CD2BP1. Although the lack of detectable FLP in the CD2BP1 immunoprecipitates herein is contrary to the results obtained with the murine homolog (Spencer *et al*., 1997), the basis of this difference remains to be determined.

The yeast two-hybrid analysis demonstrated that the SH3 domain of CD2BP1, relative to the intact CD2BP1 protein, shows only a weak interaction with the CD2 tail. This weak interaction is not peculiar to the junction formed between the B42 domain and the CD2BP1 SH3 domain in the fusion protein; various constructs included from 0 to 80 endogenous amino acids of the CD2BP1 segment immediately N-terminal to the CD2BP1 SH3 domain or, alternatively, an exogenous insertion of a glycine linker between B42 and the CD2BP1 SH3 domain, yet all yielded a weak signal. A low affinity interaction between the CD2BP1 SH3 domain and the CD2 cytoplasmic tail was also suggested by immunoprecipitation studies using T cell lysates and a GST–SH3 fusion protein coupled to Sepharose beads. Large amounts of CD2BP1 protein (i.e. mg/ml concentrations) were needed for coupling to Sepharose beads in order to discern an association with CD2. Moreover, the presence of divalent cations was required to detect an association. Given that sequences reminiscent of a cation-binding site were noted previously in the CD2 tail (Chang *et al*., 1989, 1990), a preferred configuration induced by divalent cations may be required to facilitate binding of the CD2BP1 SH3 domain to the CD2 tail. Whether the increase in intracellular free calcium following CD2 and TCR ligation enhances CD2BP1 binding physiologically is currently unknown but represents a likely possibility.

To date, two classes of proline-rich sequences with high affinity for SH3 domains have been documented (Mayer and Eck, 1995). Class I contains the motif RxxPxxP while class II contains the motif PxxPxR. These sequences permit the prolines and arginines to interact with the three binding pockets of the SH3 domain's surface. All of the proline-rich sequences in the CD2 tail, including the PPLP sequence, lack either of these motifs, perhaps explaining why the single CD2BP1 SH3 domain exhibits weak binding to CD2. The very weak interaction of the isolated CD2BP1 SH3 domain with the CD2 tail suggests that although the SH3 domain is directly involved in binding to the PPLP region of the CD2 cytoplasmic tail, other components of CD2BP1 protein may be important in promoting binding, even if only indirectly. In this regard, the PAIR COIL amino acid sequence analysis (Berger *et al*., 1995) of CD2BP1 suggests the presence of a coiled-coil structure within the N-terminal half of the protein. Proteins with coiled-coil structures often interact either among themselves or with other coiled-coil proteins through charge interactions or hydrophobic van der Waal's forces as distributed on separate surfaces of the coiled-coil helical structure (Cohen and Parry, 1990). The possibility exists, therefore, that CD2BP1 may interact with itself to form oligomers. In fact, the MULTICOIL program (Wolf *et al*., 1997) predicts the possible formation of CD2BP1 intermolecular trimers. Such oligomerization would undoubtedly increase the avidity of the SH3 domain for its binding partner on the CD2 tail (PPLP region) due to cooperative interactions resulting from the multivalency of the SH3 domains. This possibility could explain the more readily detectable binding in the yeast two-hybrid system between CD2BP1 and the CD2 tail relative to that between the isolated CD2BP1 SH3 domain and the CD2 tail. In addition, such multimerization of CD2BP1 SH3 domains would provide independent binding surfaces for several proline-rich regions, suggesting how CD2BP1 might make bridging interactions simultaneously.

Regulation of the local CD2 cytoplasmic tail concentration in the T lymphocyte could also inducibly modulate interactions with the low affinity CD2BP1 SH3 domain. The observation that CD2 co-localizes with CD2BP1 when transmembrane CD2 molecules are reorganized into clusters by CD58 suggests that this mechanism may be operative. Clustering of CD2 molecules at the cell–cell interface would result in a high local concentration of CD2 cytoplasmic tails. These in turn would associate with CD2BP1, thereby presumably delivering PTP-PEST to the area of cell–cell interaction. The phosphatase activity of PTP-PEST would then be available to regulate the CD2-mediated cell adhesion process.

It is of substantial interest that the murine CD2BP1 homolog has been shown by Wu *et al*. (1998) to bind via its SH3 domain to the murine homolog of the Wiskott–Aldrich syndrome protein (WASP). This binding apparently is regulated by phosphorylation, in particular involving SH3 residue Y367 which is conserved in both human CD2BP1 isoforms. Assuming that human CD2BP1 interacts with human WASP, then CD2BP1 binds to a minimum of two distinct proteins via its SH3 domain. How accessibility to these ligands may regulate CD2BP1 function remains to be determined.

Our current study documents the existence of two different CD2BP1 isoforms, CD2BP1L and CD2BP1S. Both proteins have an overall sequence similarity with cdc15, i.e. they possess a cdc15 homology component, a PEST-rich region and an SH3 domain. Results from yeast two-hybrid analysis suggest that both interact with the CD2 tail in the same region. However, there are differences between these proteins which could affect their function and fate. As revealed by RT–PCR, the CD2BP1S mRNA is present in low abundance compared with CD2BP1L. In addition, CD2BP1S has two continuous PEST-rich sequences while CD2BP1L has only one, making the CD2BP1S protein possibly more susceptible to degradation. If the postulated protein degradation resulted in a stable N-terminal coiled-coil and/or C-terminal SH3 domain fragment, either might negatively regulate CD2BP1 function. The CD2BP1L isoform uniquely contains a proline-rich sequence PPAP (a potential SH3-binding site), an additional tyrosine residue at amino acid 283 and a free cysteine (residue 305) which might pair with other protein components. At least under the conditions examined in T cells, however, we found no evidence for CD2BP1L covalently linked dimers. The importance of these sequence differences awaits further analysis.

The RNA expression pattern of CD2BP1 is restricted to hematopoietic cells, being distributed among T cells and NK cell populations and upregulated further in activated T cells. The distribution pattern of CD2BP1 is similar but not identical to CD2 and suggests that its biological role is relevant to T and NK cell function, presumably through interaction with CD2. Nevertheless, unlike CD2 which is expressed at a high level in the thymus, the expression of CD2BP1 is minimal in thymocytes relative to mature T

lymphocytes. This obvious difference in the RNA expression of CD2BP1 between mature and immature T cells is probably linked to the function of the gene product. As discussed above, one potentially important function of CD2BP1 is to recruit PTP-PEST to the CD2 tail, thereby resulting in downregulation of the adhesion process via regulated dephosphorylation of relevant substrates. We postulate that while this mechanism may be critical for mature T cell effector function, the requirements for thymocyte interaction with thymic stroma may be quite distinct. Prolonged adhesion in the absence of CD2BP1 may facilitate the requisite thymic stroma–thymocyte interaction involved in developmental selection processes. Further analysis of CD2BP1 function in T lineage development will test the validity of this model.

Materials and methods

Construction and screening of cDNA libraries

Human peripheral blood mononuclear cells (PBMCs) were isolated by Ficoll gradient centrifugation of peripheral blood from healthy blood donors. Activated T cells were obtained by culturing the PBMCs in RPMI-1640 containing a 1:200 dilution of 2Ad2 ascites (anti-human CD3ε mAb), 25 ng/ml PMA, 10% fetal calf serum (FCS), 1% penicillin/streptomycin, 2 mM glutamine. After 48 h of activation, ⩾94% of the residual cell population was anti-CD2 reactive as shown by FACS analysis. Total RNA was prepared from the activated T cells by the guanidine thiocyanate gradient centrifugation method (Kingston, 1987). The mRNAs were isolated from the total RNA using a polyA spin™ mRNA isolation kit (NEB). The cDNA library was synthesized using a cDNA synthesis kit (Stratagene) with an oligonucleotide containing an *Xho*I restriction site and poly(dT) at the 3′ end and ligated to an *Eco*RI adaptor at the 5′ end. After digestion with *Xho*I and *Eco*RI, the cDNAs were ligated to the yeast vector pJG4-5 (trp^+) downstream of the B42 activator ORF between the *Eco*RI and *Xho*I sites. The constructs were used to transform *Escherichia coli* strain DH12S (BRL) yielding 4×10^6 colonies. The cDNA-containing plasmids were then purified from the *E.coli* colonies and used to transform yeast EGY48 already pre-transformed with the yeast vector pSH1834 (*lacZ* reporter, ura^+) and pEG202/CD2 (his^+) (Finley and Brent, 1995). The transformants were plated on ura^-, his^-, trp^- yeast minimum medium plates and ~7×10^6 colonies were screened based on their selective growth on ura^-, his^-, trp^-, leu^- plates and blue colony color due to *lacZ* expression under galactose-induced conditions (Finley and Brent, 1995). The cDNA plasmids from positive colonies were purified and examined further for their lack of growth or *lacZ* expression when co-transformed with the yeast vector pEG202/ΔCD2 containing the LexA–CD2 tail truncation fragment. The colonies giving positive growth in ura^-, his^-, trp^-, leu^- medium or showing *lacZ* expression only when the cDNAs were co-transformed with pEG202/CD2 but not pEG202/ΔCD2 were considered significant and their cDNA inserts were subjected to DNA sequencing.

To characterize independent CD2BP1 cDNA clones, a ZAP express™ cDNA phagemid library was constructed using poly(A)$^+$ RNA from 72 h activated human T cells (obtained as above), a ZAP express™ cDNA synthesis kit and ZAP express™ cDNA gigapack II gold cloning kit (all from Stratagene). The *Xho*I fragment of CD2BP1S was labeled for library screening by random priming using [α-^{32}P]dCTP and a random primed DNA labeling kit (Boehringer Mannheim). Inserts of selected positive clones were sequenced. CD2BP1L was derived from this library.

Yeast complementation analysis of variant proteins

To examine the interaction of different truncated or mutated versions of the CD2 tail with different variants of CD2BP1, the cDNAs corresponding to each protein were generated from the original clones by PCR (Higuchi *et al*., 1988) and inserted into the relevant yeast expression vectors. For CD2 tail variants, the cDNAs were inserted in the pEG202 vector between the *Eco*RI and *Sal*I sites. For the CD2BP1 series, the cDNAs were inserted between the *Eco*RI and *Xho*I site of the pJG4-5 vector. The authenticity of all DNA constructs was confirmed by DNA sequence anlaysis. Different combinations of CD2 tail constructs and CD2BP1 constructs were used to doubly transform yeast EGY48 pre-transformed with the pSH1834 vector. The triple transformants were selected for their growth in ura^-, his^-, trp^- minimum medium. The colonies were then tested for *lacZ* expression under galactose-induced conditions. The combinations which resulted in *lacZ* expression in transformed yeast under inductive conditions were scored as a specific interaction between the CD2 tail variant and the CD2BP1 variant.

Northern analysis and 5′-rapid amplification of cDNA ends (5′-RACE) of CD2BP1

For Northern blot analysis of different human hematopoietic cell lines or the HeLa cell line, 10 μg of purified total RNA was electrophoresed on a 1% agarose gel at 80 V for 3–4 h. The separated RNAs were then transferred to Biotrans nylon membranes (ICN) in 20× SSC overnight, followed by washing in 2× SSC and baking at 80°C for 2 h. For hybridization, the *Xho*I fragment of CD2BP1S was isolated from the CD2BP1S cDNA plasmid and ^{32}P labeled. The membrane was hybridized to the labeled fragment using the ExpressHyb solution (Clontech) followed by several washes prior to autoradiography as per the manufacturer's instructions. For Northern blots of RNA from different human tissues, two human multiple tissue Northern blots were purchased from Clontech. Each lane on the membrane represents 2 μg of mRNA from different human tissues. The probing, washing and autoradiography were performed as per the manufacturer's protocol.

For 5′-RACE analysis of the cDNA sequence upstream of the existing CD2BP1 cDNA clone, a reverse primer corresponding to bp 307–326 of CD2BP1S and poly(A)$^+$ RNA purified from activated human T cells were used. The 5′-RACE system (Gibco-BRL) was used to generate dC-tailed 5′ cDNA according to the manufacturer's protocol. The first PCR was performed using the cDNA generated as template, the provided AAP oligonucleotide 5′ primer and a unique reverse primer corresponding to bp 178–202 of CD2BP1S as the 3′ primer. The second PCR was performed using the first PCR product as template, the provided UAP oligonucleotide as the 5′ primer and a unique reverse primer corresponding to bp 59–83 of CD2BP1S as 3′ primer. The second PCR product was ligated into the pCR 2.1 vector (Invitrogen) according to the manufacturer's protocol, followed by DNA sequencing analysis of the insert.

Generation of a recombinant GST–CD2BP1SH3 fusion protein and analysis of its interaction with CD2 in human T lymphocytes

To generate a GST–CD2BP1SH3 fusion protein, the cDNA sequence corresponding to amino acids 361–416 of CD2BP1L was inserted into the pGEX-4T-1 vector (Pharmacia) between the *Eco*RI and *Xho*I site in the linker region C-terminal to the GST-binding domain. The construct was used to transform *E.coli* XL2-Blue (Stratagene), and the fusion protein generated by culturing the transformed *E.coli* under isopropyl-β-D-thiogalactopyranoside (IPTG)-inducing conditions (0.1 mM IPTG for 2–3 h at 37°C). The fusion protein and/or GST control protein was then purified using glutathione–Sepharose 4B beads according to the manufacturer's protocol (Pharmacia).

To analyze the ability of the GST–CD2BP1SH3 fusion protein to interact with CD2, human T cells were purified from PBMCs by nylon wool (Hathcock, 1994) and activated for 72 h by culturing in 2Ad2 and PMA as described above. The T cells were lysed at 30×10^6 cells/ml in lysis buffer [1% Triton, 0.15 M KCl, 1× TBS (10 mM Tris pH 7.4, 0.15 M NaCl)] with or without divalent cations (Zn^{2+}, Mg^{2+} or Ca^{2+}) as indicated, supplemented with 1 mM phenylmethylsulfonyl fluoride (PMSF), 5 μg/ml leupeptin and 0.35 TIU (trypsin inhibitor unit)/ml aprotinin. Following 30 min at 4°C, the lysates were microcentrifuged for 30 min, and the supernatants pre-cleared by incubating overnight with GST–Sepharose beads (~5 mg protein/ml glutathionine–Sepharose). The pre-cleared lysates were then incubated overnight with glutathionine–Sepharose beads coupled with either the GST–CD2BP1SH3 fusion protein or GST alone (as a control). After two washes with lysis buffer (without proteinase inhibitors), the beads were incubated at 65°C for 20 min in SDS sample buffer and subjected to 12.5% SDS–PAGE. The proteins on the gel were then transferred to nitrocellulose membranes for Western blot analysis. The bound CD2 protein was then revealed by probing the membrane first with a 1:1000 dilution of polyclonal M32B rabbit anti-human CD2 (Recny *et al*., 1990) antibody pre-absorbed on bacteria lysates, followed by incubation of the membranes with horseradish peroxidase (HRP)-conjugated goat anti-rabbit antibody (Bio-Rad) at a 1:10 000 dilution. The signal was then developed by ECL (NEN). Additional experiments were conducted using lysates from hCD2wt (W33)- and ΔCD2-transfected mouse T cell hybridomas generated as previously described (Li *et al*., 1996).

Generation of mouse mAbs specific for human CD2BP1

To develop mAbs specific for CD2BP1, the purified GST–CD2BP1SH3 fusion protein was used as an immunogen. Specifically, the protein was emulsified in complete Freund's adjuvant to a final concentration of 200 μg/ml. Then 100 μg of the protein antigen was given intraperitoneally to each of several 8-week-old Balb/c mice. Subsequently, the immunized mice were boosted three more times with the same fusion protein emulsified in incomplete Freund's adjuvant. About 4×10^8 splenocytes from two immunized mice were fused to NS-1 myeloma cells, cultured in selective HAT medium and hybridoma supernatants were then screened for positive binding to the GST–CD2BP1SH3 fusion protein using standard methods (Meuer *et al*., 1984). After incubating the supernatant in 96-well plates pre-coated with GST–CD2BP1SH3 protein at 5 μg/ml, the bound mAbs were detected with alkaline phosphatase-conjugated goat anti-mouse IgG (American Qualex). The reaction was developed using the phosphatase-specific reaction with its substrate/Sigma 104 at 1 mg/ml (Sigma) in DEA buffer (49 mg $MgCl_2{\cdot}6H_2O$/l, 96 ml diethanolamine/l, pH 9.8) and the color density determined by OD reading on an ELISA reader (spectraMAX 250) at 405 nm. The supernatants from the positive hybridomas were screened further for binding to plates coated with GST protein alone under the identical conditions. Hybridomas secreting antibodies binding only to the GST–CD2BP1SH3 protein but not to GST were subcloned twice and used to generate ascites in pristane-primed Balb/C retired breeders. The mAbs were purified further from ascites by protein G (or protein A) affinity columns. The purified antibodies were coupled to CNBr-activated Sepharose 4B beads by a standard protocol (Meuer *et al*., 1984).

Fluorescence microscopy analysis of the distribution pattern of CD2BP1 and its association with CD2

To examine the distribution pattern of CD2BP1, ~2×10^6 activated human T cells were incubated with directly conjugated Texas red-labeled anti-$T11_1$ mAb (5 μg/ml) in FACS buffer [2% FCS in phosphate-buffered saline (PBS)] at 4°C for 30 min, followed by two washes in the same buffer and then fixation with 2% (w/v) paraformaldehyde/PBS for 30 min at 4°C. The cells were then permeabilized by incubation in permeabilization buffer [0.1% saponin (Sigma) in FACS buffer] at 4°C for 30 min, and stained with directly FITC-labeled anti-CD2BP1 mAb (8C93D8, 5 μg/ml) in permeabilization buffer at 4°C for 30 min. After three washes in permeabilization buffer and one wash in PBS, the cells were resuspended in 1% paraformaldehyde/PBS and analyzed under 60× magnification on a Nikon Diaphot 300 fluoromicroscope equipped with a photometric PXL cooled CCD camera linked to an Oncor imaging analysis system as described previously (Li *et al*., 1996).

For image analysis of the CD2BP1 association with CD2, CD2 molecules on the activated T cell surface were induced to cluster by either a pair of anti-CD2 antibodies (anti-$T11_2$ plus anti-$T11_3$) or by CD58 ligand-directed CD2 relocalization. For antibody cross-linking, activated T cells were incubated with anti-$T11_2$ mAb (5 μg/ml) and direct Texas red-labeled anti-$T11_3$ mAb (1:50) in FACS buffer at 4°C for 30 min, followed by two washes with FACS buffer and fixation by incubation in 2% paraformaldehyde/PBS. The cells were then permeabilized and stained with directly FITC-labeled anti-CD2BP1 mAb, followed by fluoroimaging analysis as described above. For ligand-induced surface CD2 relocalization, activated T cells were incubated with CD58-transfected CHO cells pre-bound to coverslips to induce cellular conjugate formation as described previously (Li *et al*., 1996). After washing off the non-conjugated T cells and fixation in 1% paraformaldehyde, the conjugates were stained with anti-$T11_3$ antibody (1:50) at 4°C for 30 min, followed by washing, permeabilization and staining with anti-CD2BP1 antibody as described above. The stained conjugates on the coverslips were then subjected to fluoroimaging analysis.

Protein tyrosine phosphatase characterization and activity assay

To identify the protein tyrosine phosphatase associated with CD2BP1, activated human T cells were disrupted in lysis buffer at 30×10^6/ml and the supernatant collected as described above. After pre-clearing with control beads (CNBr-activated beads linked to non-specific mouse IgG at 5 mg/ml, Sigma) overnight, the supernatant was diluted to 10×10^6 cells/ml in lysis buffer containing 0.1% bovine serum albumin (BSA). CD2BP1 and any associated molecules were immunoprecipitated by incubation at 4°C for 3 h with CNBr beads coupled to either anti-CD2BP1 mAb 8C93D8 or, as a control, non-specific mouse IgG. After two washes in lysis buffer and one wash in TBS, the immunocomplexes on the beads were eluted by heating at 65°C for 20 min in SDS sample buffer and subjected to 12.5% reducing SDS–PAGE. After electrophoresis, proteins on the gel were transferred to nitrocellulose for Western blotting. The membranes were then probed with different primary antibodies: rabbit anti-human PTP-PEST (CSH8) 1:1000 (Garton and Tonks, 1994), rabbit anti-human FLP (αEN12) 1:1000 (Dosil *et al*., 1996), goat anti-human SHPTP1 (Santa Cruz) 1:100 or rabbit anti-human SHPTP2 (Santa Cruz) 1:100, followed by washing and incubation with the secondary HRP-conjugated goat anti-rabbit antibody (1:5000) or donkey anti-goat antibody (Santa Cruz) 1:2000, and signals developed by ECL.

In vitro protein tyrosine phosphatase assay. After immunoprecipitation as described above, the 8C93D8 beads or control beads were washed once with lysis buffer containing 0.5% sodium deoxycholate (DOC), 0.5 M NaCl and 0.1% BSA, followed by washing with lysis buffer containing 0.5% DOC, 0.1% SDS and 0.1% BSA, and finally two washes with 50 mM Tris, pH 7.5, 0.15% 2-mercaptoenthanol, 0.0075% Brij 35 and 0.025 mM EDTA. The immunocomplex bound on the beads was assayed for the protein tyrosine phosphatase activity on ^{32}P-labeled tyr Raytide as measured by the ^{32}P release from the peptide using a previously established protocol (Tsai *et al*., 1991). ^{32}P labeling of Raytide at the tyrosine residue was carried out using an established kinase reaction procedure (Tsai *et al*., 1991) with the synthetic peptide Raytide as substrate (Calbiochem), [γ-^{32}P]ATP (NEN) as the ^{32}P donor and v-abl as the tyrosine kinase (Calbiochem). After incubation at 37°C for 5 h, the ^{32}P-labeled Raytide was precipitated twice by trichloroacetic acid (TCA) and the substrate was finally dissolved in 0.2 M Tris, pH 8.0 for phosphatase assay as described (Tsai *et al*., 1991).

In vitro kinase assay. Immunoprecipitation was performed as described above except using a modified lysis buffer containing 1 mM Na_3VO_4, 5 mM $Na_2H_2P_2O_7$ and 5 mM NaF in addition to the other components. The beads were then washed twice with lysis buffer and twice with kinase buffer (100 mM NaCl, 5 mM $MnCl_2$, 5 mM $MgCl_2$, 20 mM HEPES, pH 7.4). The kinase reaction was conducted in 50 μl of kinase buffer containing 2 μM ATP, 10 μCi of [γ-^{32}P]ATP and 10 μg of one of the following kinase substrates: histone H1 (Calbiochem), poly(GluTyr) (Sigma) or Raytide (Calbiochem). After 15 min incubation at room temperature, the reaction was terminated by boiling in SDS sample buffer, followed by either 9% SDS–PAGE or spotting onto P81 phosphocellulose paper (Gibco-BRL), followed by three washes with 0.5% phosphoric acid. The results were analyzed by autoradiography.

COS cell CD2 adhesion assay and immunoprecipitation studies

A total of 2×10^5 COS7 cells were seeded onto 6-well tissue culture plates. After overnight culture, each well was transfected with 5 μg of control DNA (pcDNA1.1) (Invitrogen) or 0.5 μg of CD2/CDM8 (Arulanandam *et al*., 1993b) along with various amounts of CD2BP1L/pcDNA1.1. In the latter construct, PCR was used to append a FLAG sequence to the N-terminus of CD2BP1L. The transfection was performed using established calcium phosphate precipitation methods. After 48 h expression, COS7 cells were washed twice with Dulbecco's modified Eagle's medium (DMEM) and incubated with 2-aminoethylisothiouronium bromide (AET)-treated SRBCs for 1 h at room temperature as previously described (Arulanandam *et al*., 1993a). After washing off the unbound SRBCs, rosettes were counted. Rosetting of cells singularly transfected with either wtCD2 or ΔCD2 CD2 cDNA cloned into the CDM8 vector was taken as 100% standard. The rosette-positive double transfectants (CD2 plus CD2BP1L) were then counted and expressed as a percentage related to transfectants with wtCD2 or ΔCD2 alone.

About 10^6 COS7 cells were seeded onto 100 mm plates (Falcon). After 24 h, 16 μg of N-terminal FLAG-tagged CD2BP1/pcDNA1.1 was co-transfected with 4 μg of wtCD2, ΔCD2 or CD4 by the method of calcium phosphate precipitation. After 48 h of expression, cells were lysed at 20×10^6/ml in lysis buffer containing 250 μM $ZnCl_2$ as described above. The lysis supernatants were pre-cleared with non-specific mouse IgG-coupled Sepharose 4B beads, diluted 1:5 and immunoprecipitated with 3T48B5-, 8C93D8- or anti-CD4 (19Thy5D2)-coupled Sepharose 4B beads. The immunocomplexes were washed three times with lysis buffer and subjected to 9% SDS–PAGE and Western blot analysis.

Time-lapse video microscopy of stable CD2BP1-positive and CD2BP1-negative transfectants

To generate a stable J77 line expressing CD2BP1L, CD2BP1L cDNA were inserted into the pPINK-2 vector between the *Xba*I and *Bam*HI sites. A 20 μg aliquot of the construct was used to transfect 10^7 Jurkat 77 cells by electroporation using 800 μF and 250 V. Transfected cells

were cultivated under 1.5 mg/ml G418 selection in culture media (RPMI-1640 supplemented with 10% FCS, 1% penicillin streptomycin and 2 mM glutamine) at 2×10^5 cells/well. Expression of CD2BP1L in transfectants was confirmed both by intracellular staining analysis by FACS using anti-CD2BP1 and by Northern blot analysis. Positive transfectants were maintained with 0.5 mg/ml G418 in the culture media. A control G418-resistant cell line derivation of J77 termed D5, which lacks CD2BP1 expression, was maintained under identical conditions.

Cells were culture at 1×10^6/ml on plates coated with fibronectin as previously described (Salgia *et al*., 1997) in a temperature- and CO_2-controlled chamber in RPMI-1640 supplemented with 10% FCS, 1% penicillin–streptomycin, 2 mM glutamine and 0.5 mg/ml G418. The cells, with and without stimulation, were examined utilizing an Olympus IX70 inverted microscope, Omega temperature control device, Optronics Engineering DEI-750 3CCD digital video camera and a Sony SVT-S3100 time-lapse S-VHS video recorder. For image presentation, video images were captured and printed with a Sony Color Video Printer UP-5600 MD. Images were printed for every 10 min interval.

Acknowledgements

The authors thank Dr B.Neel for helpful suggestions, Dr J.Ritz for providing the NKL cell line and Drs N.Tonks and I.Lemischka for antisera to PTP-PEST and FLP, respectively. We thank Drs J.Griffin and L.Clayton for review of the manuscript. The DNA sequences have been deposited in DDBJ/EMBL/GenBank under accession numbers AF038602 for CD2BP1S and AF038603 for CD2BP1L. This work was supported by NIH grant AI21226 to E.L.R. K.N. greatly acknowledges funding support from Dr S.Okinaga.

References

Altschul,S.F., Gish,W., Miller,W., Myers,E.W. and Lipman,D.J. (1990) Basic local alignment search tool. *J. Mol. Biol.*, **215**, 403–410.

Arulanandam,A.R.N., Moingeon,P., Concino,M.F., Recny,M.A., Kato,K., Yagita,H., Koyasu,S. and Reinherz,E.L. (1993a) A soluble multimeric recombinant CD2 protein identifies CD48 as a low affinity ligand for human CD2: divergence of CD2 ligands during the evolution of humans and mice. *J. Exp. Med.*, **177**, 1439–1450.

Arulanandam,A.R.N., Withka,J.M., Wyss,D.F., Wagner,G., Kister,A., Pallai,P., Recny,M.A. and Reinherz,E.L. (1993b) The CD58 (LFA-3) binding site is a localized and highly charged surface area on the AGFCC′C″ face of the human CD2 adhesion domain. *Proc. Natl Acad. Sci. USA*, **90**, 11613–11617.

Arulanandam,A.R.N., Kister,A., McGregor,M.J., Wyss,D.F., Wagner,G. and Reinherz,E.L. (1994) Interaction between human CD2 and CD58 involves the major β-sheet surfaces of each of their respective adhesion domains. *J. Exp. Med.*, **180**, 1861–1871.

Astier,A., Avraham,H., Manie,S.N., Groopman,J., Canty,T., Avraham,S. and Freedman,A.S. (1997) The related adhesion focal tyrosine kinase is tyrosine-phosphorylated after β1-integrin stimulation in B cells and binds to p130cas. *J. Biol. Chem.*, **272**, 228–232.

Bell,G.M., Fargnoli,J., Bolen,J.B., Kish,L. and Imboden,J.B. (1996) The SH3 domain of p56lck binds to proline-rich sequences in the cytoplasmic domain of CD2. *J. Exp. Med.*, **183**, 169–178.

Berger,B., Wilson,D.B., Wolf,E., Tonchev,T., Milla,M. and Kim,P.S. (1995) Predicting coiled coils by use of pairwise residue correlations. *Proc. Natl Acad. Sci. USA*, **92**, 8259–8263.

Bergman,M., Joukov,V., Virtanen,I. and Alitalo,K. (1995) Overexpressed csk tyrosine kinase is localized in focal adhesions, causes reorganization of αvβ5 integrin and interferes with HeLa cell spreading. *Mol. Cell. Biol.*, **15**, 711–722.

Bierer,B.E., Peterson,A., Gorga,J.C., Herrmann,S.H. and Burakoff,S.J. (1988) Synergistic T cell activation via the physiological ligands for CD2 and the T cell receptor. *J. Exp. Med.*, **168**, 1145–1156.

Bierer,B.E., Sleckman,B.P., Ratnofsky,S.E. and Burakoff,S.J. (1989) The biologic roles of CD2, CD4 and CD8 in T cell activation. *Annu. Rev. Immunol.*, **7**, 579–599.

Black,D.S. and Bliska,J.B. (1997) Identification of p130cas as a substrate of *Yersinia* YopH (Yop51), a bacterial protein tyrosine phosphatase that translocates into mammalian cells and targets focal adhesions. *EMBO J.*, **16**, 2730–2744.

Bodian,D.L., Jones,E.Y., Harlos,K., Stuart,D.I. and Davis,S.J. (1994) Crystal structure of the extracellular region of the human cell adhesion molecule CD2 at 2.5 Å resolution. *Structure*, **2**, 755–766.

Boussiotis,V.A., Freeman,G.J., Griffin,J.D., Gray,G.S., Gribben,J.G. and Nadler,L.M. (1994) CD2 is involved in maintenance and reversal of human alloantigen-specific clonal anergy. *J. Exp. Med.*, **180**, 1665–1673.

Chang,H.-C., Moingeon,P., Lopez,P., Krasnow,H., Stebbins,C. and Reinherz,E.L. (1989) Dissection of the human CD2 intracellular domain: identification of a segment required for signal transduction and interleukin 2 production. *J. Exp. Med.*, **169**, 2073–2083.

Chang,H.-C., Moingeon,P., Pedersen,R., Lucich,J., Stebbins,C. and Reinherz,E.L. (1990) Involvement of the PPPGHR motif in T cell activation via CD2. *J. Exp. Med.*, **172**, 351–355.

Charest,A., Wagner,J., Jacob,S., McGlade,J. and Tremblay,M.L. (1996) Phosphotyrosine-independent binding of SHC to the NPLH sequence of murine protein-tyrosine phosphatase-PEST. *J. Biol. Chem.*, **271**, 8424–8429.

Charest,A., Wagner,J., Kwan,M. and Tremblay,M.L. (1997) Coupling of the murine protein tyrosine phosphatase PEST to the epidermal growth factor (EGF) receptor through a Src homology 3 (SH3) domain-mediated association with Grb2. *Oncogene*, **14**, 1643–1651.

Cheng,J., Daimaru,L., Fennie,C. and Lasky,L.A. (1996) A novel protein tyrosine phosphatase expressed in $lin^{lo}CD34^{hi}Sca^{hi}$ hematopoietic progenitor cells. *Blood*, **88**, 1156–1167.

Chow,L.M.L., Fournel,M., Davidson,D. and Veillette,A. (1993) Negative regulation of T cell receptor signaling by tyrosine protein kinase p50csk. *Nature*, **365**, 156–160.

Clayton,L.K., Sayre,P.H., Novotny,J. and Reinherz,E.L. (1987) Murine and human T11 (CD2) cDNA sequences suggest a common signal transduction mechanism. *Eur. J. Immunol.*, **17**, 1367–1370.

Cloutier,J.-F., Chow,L.M.L. and Veillette,A. (1995) Requirement of the SH3 and SH2 domains for the inhibitory function of tyrosine protein kinase p50csk in T lymphocytes. *Mol. Cell. Biol.*, **15**, 5937–5944.

Cohen,C. and Parry,D.A.D. (1990) α-Helical coiled coils and bundles: how to design an α-helical protein. *Proteins: Struct. Funct. Genet.*, **7**, 1–15.

Davidson,D., Cloutier,J.-F., Gregorieff,A. and Veillette,A. (1997) Inhibitory tyrosine protein kinase p50csk is associated with protein tyrosine phosphatase PTP-PEST in hematopoietic and non-hematopoietic cells. *J. Biol. Chem.*, **272**, 23455–23462.

Dosil,M., Leibman,N. and Lemischka,I.R. (1996) Cloning and characterization of fetal liver phosphatase 1, a nuclear protein tyrosine phosphatase isolated from hematopoietic stem cells. *Blood*, **88**, 4510–4525.

Dowbenko,D., Spencer,S., Quan,C. and Lasky,L.A. (1998) Identification of a novel polyproline recognition site in the cytoskeletal associated protein, proline serine threonine phosphatase interacting protein. *J. Biol. Chem.*, **273**, 989–996.

Driscoll,P.C., Cyster,J.G., Campbell,I.D. and Williams,A.F. (1991) Structure of domain 1 of rat T lymphocyte CD2 antigen. *Nature*, **353**, 762–765.

Fankhauser,C., Reymond,A., Cerutti,L., Utzig,S., Hofmann,K. and Simanis,V. (1995) The *S.pombe cdc15* gene is a key element in the reorganization of F-actin at mitosis. *Cell*, **82**, 435–444.

Finley,R.L. and Brent,R. (1995) Interaction trap cloning with yeast. In Glover,D.M. and Hames,B.D. (eds), *DNA Cloning 2, Expression Systems. A Practical Approach.* IRL Press at Oxford University Press, pp. 169–203.

Freeman,R.M., Plutzky,J. and Neel,B.G. (1992) Identification of a human src homology 2-containing protein-tyrosine-phosphatase: a putative homolog of *Drosophila* corkscrew. *Proc. Natl Acad. Sci. USA*, **89**, 11239–11243.

Garton,A.J. and Tonks,N.K. (1994) PTP-PEST: a protein tyrosine phosphatase regulated by serine phosphorylation. *EMBO J.*, **13**, 3763–3771.

Garton,A.J., Flint,A.J. and Tonks,N.K. (1996) Identification of p130cas as a substrate for the cytosolic protein tyrosine phosphatase PTP-PEST. *Mol. Cell. Biol.*, **16**, 6408–6418.

Garton,A.J., Burnham,M.R., Bouton,A.H. and Tonks,N.K. (1997) Association of PTP-PEST with the SH3 domain of p130cas: a novel mechanism of protein tyrosine phosphatase substrate regulation. *Oncogene*, **15**, 877–885.

Gassmann,M., Amrein,K.E., Flint,N.A., Schraven,B. and Burn,P. (1994) Identification of a signaling complex involving CD2, ζ chain and p59*fyn* in T lymphocytes. *Eur. J. Immunol.*, **24**, 139–144.

Gollob,J.A., Li,J., Reinherz,E.L. and Ritz,J. (1995) CD2 regulates responsiveness of activated T cells to interleukin 2. *J. Exp. Med.*, **182**, 721–731.

Gollob,J.A., Li,J., Kawasaki,H., Daley,J.F., Groves,C., Reinherz,E.L. and Ritz,J. (1996) Molecular interaction between CD58 and CD2 counter-receptors mediates the ability of monocytes to augment T cell activation by IL-12. *J. Immunol.*, **157**, 1886–1893.

Group,G.C. (1991) Multiple sequence analysis, pile up. *GCG Sequence Analysis Software Package 7*.

Guruprasad,L., Dhanaraj,V., Timm,D., Blundell,T.L., Gout,I. and Waterfield,M.D. (1995) The crystal structure of the N-terminal SH3 domain of Grb2. *J. Mol. Biol.*, **248**, 856–866.

Habib,T., Herrera,R. and Decker,S.J. (1994) Activators of protein kinase C stimulate association of Shc and the PEST tyrosine phosphatase. *J. Biol. Chem.*, **269**, 25243–25246.

Hahn,W.C. and Bierer,B.E. (1993) Separable portions of the CD2 cytoplasmic domain involved in signaling and ligand avidity regulation. *J. Exp. Med.*, **178**, 1831–1836.

Hathcock,K.S. (1994) T cell enrichment by nonadherence to nylon. In Coligan,J.E., Kruisbeek,A.M., Margulies,D.H., Shevach,E.M. and Strober,W. (eds), *Current Protocols in Immunology.* John Wiley & Sons, New York.

Higuchi,R., Krummel,B. and Saiki,R.K. (1988) A general method of *in vitro* preparation and specific mutagenesis of DNA fragments: study of protein and DNA interactions. *Nucleic Acids Res.*, **16**, 7351–7367.

Howell,B.W. and Cooper,J.A. (1994) Csk suppression of src involves movement of csk to sites of src activity. *Mol. Cell. Biol.*, **14**, 5402–5411.

Ihle,J.N., Witthuhn,B.A., Qelle,F.W., Yamamoto,K. and Silvennoinen,O. (1995) Signaling through the hematopoietic cytokine receptors. *Annu. Rev. Immunol.*, **13**, 369–398.

Jones,E.Y., Davis,S.J., Williams,A.F., Harlos,K. and Stuart,D.I. (1992) Crystal structure at 2.8Å resolution of a soluble form of the cell adhesion molecule CD2. *Nature*, **360**, 232–239.

Kanner,S.B., Reynolds,A.B., Wang,H.-C.R., Vines,R.R. and Parsons,J.T. (1991) The SH2 and SH3 domains of pp60src direct stable association with tyrosine phosphorylated proteins p130 and p110. *EMBO J.*, **10**, 1689–1698.

Kingston,R.E. (1987) Preparation and analysis of RNA: guanidinium method for total RNA preparation. In Ausubel,F.M., Brent,R., Kingston,R.E., Moore,D.D., Seidman,J.G., Smith,J.A. and Struhl,K. (eds), *Current Protocols in Molecular Biology.* Greene Publishing & Wiley-Interscience, New York.

Koyasu,S., Lawton,T., Novick,D., Recny,M.A., Siliciano,R.F., Wallner,B.P. and Reinherz,E.L. (1990) Role of interaction of CD2 molecules with lymphocyte function-associated antigen 3 in T cell recognition of normal antigen. *Proc. Natl Acad. Sci. USA*, **87**, 2603–2607.

Krensky,A.M., Sanchez-Madrid,F., Robbins,E., Nagy,J.A., Springer,T.A. and Burakoff,S.J. (1983) The functional significance, distribution and structure of LFA-1, LFA-2 and LFA-3: cell surface antigens associated with CTL-target interactions. *J. Immunol.*, **131**, 611–616.

Li,J., Smolyar,A., Sunder-Plassmann,R. and Reinherz,E.L. (1996) Ligand-induced conformational change within the CD2 ectodomain accompanies receptor clustering: implication for molecular lattice formation. *J. Mol. Biol.*, **263**, 209–226.

Liu,F., Hill,D.E. and Chernoff,J. (1996) Direct binding of the proline-rich region of protein tyrosine phosphatase 1B to the src homology 3 domain of p130cas. *J. Biol. Chem.*, **271**, 31290–31295.

Matsuzaki,Y., Gyotoku,J., Ogawa,M., Nishikawa,S., Katsura,Y., Gachelin,G. and Nakauchi,H. (1993) Characterization of c-kit positive intrathymic stem cells that are restricted to lymphoid differentiation. *J. Exp. Med.*, **178**, 1283–1292.

Matthews,R.J., Bowne,D.B., Flores,E. and Thomas,M.L. (1992) Characterization of hematopoietic intracellular protein tyrosine phosphatases: description of a phosphatase containing an SH2 domain and another enriched in proline, glutamic acid, serine and threonine-rich sequences. *Mol. Cell. Biol.*, **12**, 2396–2405.

Mayer,B.J. and Eck,M.J. (1995) Minding your p's and q's. *Curr. Biol.*, **5**, 364–367.

Mayer,B.J. and Hanafusa,H. (1990) Mutagenic analysis of the v-*crk* oncogene: requirement for SH2 and SH3 domains and correlation between increased cellular phosphotyrosine and transformation. *J. Virol.*, **64**, 3581–3589.

Meuer,S.C. *et al*. (1984) An alternative pathway of T cell activation: a functional role for the 50 kD T11 sheep erythrocyte receptor protein. *Cell*, **36**, 897–906.

Moingeon,P., Chang,H.-C., Sayre,P.H., Clayton,L.K., Alcover,A., Gardner,P. and Reinherz,E.L. (1989a) The structural biology of CD2. *Immunol. Rev.*, **111**, 111–144.

Moingeon,P., Chang,H.-C., Wallner,B.P., Stebbins,C., Frey,A.Z. and Reinherz,E.L. (1989b) CD2-mediated adhesion facilitates T lymphocyte antigen recognition function. *Nature*, **339**, 312–314.

Musacchio,A., Wilmannis,M. and Saraste,M. (1994) Structure and function of the SH3 domain. *Prog. Biophys. Mol. Biol.*, **61**, 283–297.

Nakamoto,T., Sakai,R., Honda,H., Ogawa,S., Ueno,H., Suzuki,T., Aizawa,S.-I., Yazaki,Y. and Hirai,H. (1997) Requirements for localization of p130cas to focal adhesion. *Mol. Cell. Biol.*, **17**, 3884–3897.

Nojima,Y. *et al*. (1995) Integrin-mediated cell adhesion promotes tyrosine phosphorylation of p130cas, a src homology 3-containing molecule having multiple src homology 2-binding motifs. *J. Biol. Chem.*, **270**, 15398–15402.

Osborn,L., Day,E.S., Miller,G.T., Karpusas,M., Tizard,R., Meuer,S.C. and Hochman,P.S. (1995) Amino acid residues required for binding of lymphocyte function-associated antigen 3 (CD58) to its counter-receptor. *J. Exp. Med.*, **181**, 429–434.

Peterson,A. and Seed,B. (1987) Monoclonal antibody and ligand binding sites of the T cell erythrocyte receptor (CD2) *Nature*, **329**, 842–846.

Petruzzelli,L., Takami,M. and Herrera,R. (1996) Adhesion through the interaction of lymphocyte function-associated antigen-1 with intracellular adhesion molecule-1 induces tyrosine phosphorylation of p130cas and its association with c-CrkII. *J. Biol. Chem.*, **271**, 7796–7801.

Plutzky,J., Neel,B.G. and Rosenberg,R.D. (1992) Isolation of a src homology 2-containing tyrosine phosphatase. *Proc. Natl Acad. Sci. USA*, **89**, 1123–1127.

Rechsteiner,M. and Rogers,S.W. (1996) PEST sequences and regulation by proteolysis. *Trends Biochem. Sci.*, **21**, 267–271.

Recny,M.A., Neidardt,E.A., Sayre,P.H., Ciardelli,T.L. and Reinherz,E.L. (1990) Structural and functional characterization of the CD2 immunoadhesion domain. *J. Biol. Chem.*, **265**, 8542–8549.

Sabe,H., Hata,A., Okada,M., Nakagawa,H. and Hanafusa,H. (1994) Analysis of the binding of the src homology 2 domain of csk to tyrosine-phosphorylated proteins in the suppression and mitotic activation of c-src. *Proc. Natl Acad. Sci. USA*, **91**, 3984–3988.

Sakai,R., Iwamatsu,A., Hirano,N., Ogawa,S., Tanaka,T., Mano,H., Yazaki,Y. and Hirai,H. (1994) A novel signaling molecule, p130, forms stable complexes *in vivo* with v-Crk and v-Src in a tyrosine phosphorylation dependent manner. *EMBO J.*, **13**, 3748–3756.

Salgia,R. *et al*. (1996) p130cas forms a signaling complex with the adapter protein CRKL in hematopoietic cells transformed by the BCR/ABL oncogene. *J. Biol. Chem.*, **271**, 25198–25203.

Sanchez-Madrid,F., Krensky,A.M., Ware,C.F., Robbins,E., Strominger,J.L. and Burakoff,S.J. (1982) Three distinct antigens associated with human T lymphocyte-mediated cytolysis: LFA-1, LFA-2 and LFA-3. *Proc. Natl Acad. Sci. USA*, **79**, 7489–7493.

Sayre,P.H., Chang,H.-C., Hussey,R.E., Brown,N.R., Richardson,N.E., Spagnoli,G., Clayton,L.K. and Reinherz,E.L. (1987) Molecular cloning and expression of T11 cDNA reveal a receptor-like structure on human T lymphocytes. *Proc. Natl Acad. Sci. USA*, **84**, 2941–2945.

Sayre,P.H., Hussey,R.E., Chang,H.-C., Ciardelli,T.L. and Reinherz,E.L. (1989) Structural and binding analysis of a two domain extracellular CD2 molecule. *J. Exp. Med.*, **169**, 995–1009.

Schlaepfer,D.D. and Hunter,T. (1997) Focal adhesion kinase overexpression enhances ras-dependent integrin signaling to ERK2/mitogen-activated protein kinase through interactions with and activation of c-src. *J. Biol. Chem.*, **272**, 13189–13195.

Schlaepfer,D.D., Hanks,S.K., Hunter,T. and van der Geer,P. (1994) Integrin-mediated signal transduction linked to Ras pathway by GRB2 binding to focal adhesion kinase. *Nature*, **372**, 786–791.

Seed,B. and Aruffo,A. (1987) Molecular cloning of the CD2 antigen, the T cell erythrocyte receptor, by a rapid immunoselection procedure. *Proc. Natl Acad. Sci. USA*, **84**, 3365–3369.

Selvaraj,P., Plunkett,M.L., Dustin,M., Sanders,M.E., Shaw,S. and Springer,T.A. (1987) The T lymphocyte glycoprotein CD2 binds the cell surface ligand LFA-3. *Nature*, **326**, 400–403.

Shimizu,Y., Mobley,J.L., Finkelstein,L.D. and Chan,A.S. (1995) A role for phosphatidylinositol 3-kinase in the regulation of beta 1 integrin activity by the CD2 antigen. *J. Cell Biol.*, **131**, 1867–1880.

Siliciano,R.F., Pratt,J.C., Schmidt,R.E., Ritz,J. and Reinherz,E.L. (1985) Activation of cytolytic T lymphocyte and natural killer cell function through the T11 sheep erythrocyte binding protein. *Nature*, **317**, 428–430.

Somoza,C., Driscoll,P.C., Cyster,J.G. and Williams,A.F. (1993) Mutational analysis of the CD2/CD58 interaction: the binding site for CD58 lies on one face of the first domain of human CD2. *J. Exp. Med.*, **178**, 549–558.

Spencer,S., Dowbenko,D., Cheng,J., Li,W., Brush,J., Utzig,S., Simanis,V. and Lasky,L.A. (1997) PSTPIP: a tyrosine phosphorylated cleavage furrow-associated protein that is a substrate for a PEST tyrosine phosphatase. *J. Cell Biol.*, **138**, 845–860.

Springer,T.A. (1990) Adhesion receptors of the immune system. *Nature*, **346**, 425–434.

Swain,S.L. and Cambier,J.C. (1996) Lymphocyte activation and effector function. *Curr. Opin. Immunol.*, ***8***, 309–444.

Tavernor,A.S., Kydd,J.H., Bodian,D.L., Jones,E.Y., Stuart,D.I., Davis,S.J. and Butcher,G.W. (1994) Expression cloning of an equine T lymphocyte glycoprotein CD2 cDNA structure-based analysis of conserved sequence elements. *Eur. J. Biochem.*, **219**, 969–976.

Tobe,K. *et al*. (1996) Csk enhances insulin-stimulated dephosphorylation of focal adhesion proteins. *Mol. Cell. Biol.*, **16**, 4765–4772.

Tsai,A.Y.M., Itoh,M., Streuli,M., Thai,T. and Saito,H. (1991) Isolation and characterization of temperature-sensitive and thermostable mutants of the human receptor-like protein tyrosine phosphatase LAR. *J. Biol. Chem.*, **266**, 10534–10543.

van der Merwe,P.A., Barclay,A.N., Mason,D.W., Davies,E.A., Morgan,P., Tone,M., Krishnam,A.K.C., Ianelli,C. and Davis,S.J. (1994) Human cell adhesion molecule CD2 binds CD58 (LFA-3) with a very low affinity and an extremely fast dissociation rate but does not bind CD48 or CD59. *Curr. Biol.*, **5**, 74–84.

Vuori,K. and Ruoslahti,E. (1995) Tyrosine phosphorylation of p130cas and cortactin accompanies integrin-mediated cell adhesion to extracellular matrix. *J. Biol. Chem.*, **270**, 22259–22262.

Vuori,K., Hirai,H., Aizawa,S. and Ruoslahti,E. (1996) Induction of p130cas signaling complex formation upon integrin-mediated cell adhesion: a role for src family kinases. *Mol. Cell. Biol.*, **16**, 2606–2613.

Wingren,A.G. *et al*. (1993) Monocyte-regulated IFN-γ production in human T cells involves CD2 signaling. *J. Immunol.*, **151**, 1328–1336.

Withka,J.M., Wyss,D.F., Wagner,G., Arulanandam,A.R.N., Reinherz,E.L. and Recny,M.A. (1993) Structure of the glycosylated adhesion domain of human T lymphocyte glycoprotein CD2. *Structure*, **1**, 69–81.

Wolf,E., Kim,P.S. and Berger,B. (1997) Multi-coil: a program for predicting two and three-stranded coiled coils. *Protein Sci.*, **6**, 1179–1189.

Wu,Y., Spencer,S.D. and Lasky,L.A. (1998) Tyrosine phosphorylation regulates the SH3-mediated binding of the Wiskott–Aldrich syndrome protein to PSTPIP, a cytoskeletal associated protein. *J. Biol. Chem.*, **273**, 5765–5770.

Yang,S.Y., Chouaib,S. and Dupont,B. (1986) A common pathway for T lymphoycte activation involving both the CD3–Ti complex and CD2 sheep erythrocyte receptor determinants. *J. Immunol.*, **137**, 1097–1100.

Received August 21, 1998; revised October 19, 1998; accepted October 20, 1998

Note added in proof

Since this manuscript was submitted, an independent study by Dustin and colleagues has appeared (Dustin *et al*., *Cell*, **94**, 667–677, 1998). Interestingly, the authors have identified another SH3-containing adaptor protein (CD2AP) unrelated to CD2BP1, which binds to the same CD2 cytoplasmic tail segment (amino acids 300–309) and influences focal capping and cell polarity. How CD2AP and CD2BP1 regulate each other's function remains to be determined.